Chapter 2

Introduction and Physics Motivation

2.1 Introduction

This chapter gives the physics context of magnetic moment measurements, the Standard Model expectations, along with the reach of such experiments to identify and constrain physics beyond the Standard Model. Except for a broad-brush mention of the experimental technique, the details are left for later chapters. Chapter 3 gives an overview of the experimental method, and the subsequent chapters give the details. We attempt to follow the WBS structure in those later chapters.

2.2 Magnetic and Electric Dipole Moments

The study of magnetic moments of subatomic particles grew up with the development of quantum mechanics. For fermions the magnetic dipole moment (MDM) is related to the spin by

$$\vec{\mu} = g\frac{Qe}{2m}\vec{s}. \tag{2.1}$$

where $Q = \pm 1$ and $e > 0$. Our modern interpretation of the Stern-Gerlach experiments [1, 2] is that their observation: "to within 10% the magnetic moment of the silver atom is one Bohr magneton" was telling us that the g-factor of the un-paired electron is equal to 2. However, reaching this conclusion required the discovery of spin [3], quantum mechanics [4] along with with Thomas' relativistic correction [5]. Phipps and Taylor [6] repeated the Stern-Gerlach experiment in hydrogen, and mentioned the electron spin explicitly. One of the great successes of Dirac's relativistic theory [7] was the prediction that $g \equiv 2$.

For some years, the experimental situation remained the same. The electron had $g = 2$, and the Dirac equation seemed to describe nature. Then a surprising and completely unexpected result was obtained. In 1933, against the advice of Pauli who believed that the proton was a pure Dirac particle [8], Stern and his collaborators [9] showed that the g-factor of the proton was ~ 5.5, not the expected value of 2. Even more surprising was the discovery in 1940 by Alvarez and Bloch [10] that the neutron had a large magnetic moment.

In 1947, motivated by measurements of the hyperfine structure in hydrogen that obtained splittings larger than expected from the Dirac theory [11, 12, 13], Schwinger [51] showed that

from a theoretical viewpoint these "discrepancies can be accounted for by a small additional electron spin magnetic moment" that arises from the lowest-order radiative correction to the Dirac moment[1],

$$\frac{\delta\mu}{\mu} = \frac{1}{2\pi}\frac{e^2}{\hbar c} = 0.001162. \tag{2.2}$$

It is useful to break the magnetic moment into two terms:

$$\mu = (1+a)\,\frac{e\hbar}{2m}, \quad \text{where} \quad a = \frac{(g-2)}{2}. \tag{2.3}$$

The first term is the Dirac moment, 1 in units of the appropriate magneton $e\hbar/2m$. The second term is the anomalous (Pauli) moment [14], where the dimensionless quantity a (Schwinger's $\delta\mu/\mu$) is sometimes referred to as the *anomaly*.

2.2.1 The Muon

The muon was first observed in a Wilson cloud chamber by Kunze[15] in 1933, where it was reported to be "a particle of uncertain nature." In 1936 Anderson and Neddermeyer[16] reported the presence of "particles less massive than protons but more penetrating than electrons" in cosmic rays, which was confirmed in 1937 by Street and Stevenson[17], Nishina, Tekeuchi and Ichimiya[18], and by Crussard and Leprince-Ringuet[19]. The Yukawa theory of the nuclear force had predicted such a particle, but this "mesotron" as it was called, interacted too weakly with matter to be the carrier of the strong force. Today we understand that the muon is a second generation lepton, with a mass about 207 times the electron's. Like the electron, the muon obeys quantum electrodynamics, and can interact with other particles through the electromagnetic and weak forces. Unlike the electron which appears to be stable, the muon decays through the weak force predominantly by $\mu^- \to e^-\nu_\mu\bar{\nu}_e$. The muon's long lifetime of $\simeq 2.2$ μs permits precision measurements of its mass, lifetime, and magnetic moment.

2.2.2 The Muon Magnetic Moment

The magnetic moment of the muon played an important role in the discovery of the generation structure of the Standard Model (SM). The pioneering muon spin rotation experiment at the Nevis cyclotron observed parity violation in muon decay [20], and also showed that g_μ was consistent with 2. Subsequent experiments at Nevis [22] and CERN [23] showed that $a_\mu \simeq \alpha/(2\pi)$, implying that in a magnetic field, the muon behaves like a heavy electron. Two additional experiments at CERN required that contributions from higher-order QED [24], and then from virtual hadrons [25] be included into the theory in order to reach agreement with experiment.

2.2.3 The Muon Electric Dipole Moment

Dirac [7] discovered an electric dipole moment (EDM) term in his relativistic electron theory. Like the magnetic dipole moment, the electric dipole moment must be along the spin. We

[1] A misprint in the original paper has been corrected here.

can write an EDM expression similar to Eq. (2.1),

$$\vec{d} = \eta \left(\frac{Qe}{2mc} \right) \vec{s}, \tag{2.4}$$

where η is a dimensionless constant that is analogous to g in Eq. (2.1). While magnetic dipole moments (MDMs) are a natural property of charged particles with spin, electric dipole moments (EDMs) are forbidden both by parity and by time reversal symmetry.

The search for an EDM dates back to the suggestion of Purcell and Ramsey [26] in 1950, well in advance of the paper by Lee and Yang [27], that a measurement of the neutron EDM would be a good way to search for parity violation in the nuclear force. An experiment was mounted at Oak Ridge [28] soon thereafter that placed a limit on the neutron EDM of $d_n < 5 \times 10^{-20}$ e-cm, although the result was not published until after the discovery of parity violation.

Once parity violation was established, Landau [29] and Ramsey [30] pointed out that an EDM would violate both P and T symmetries. This can be seen by examining the Hamiltonian for a spin one-half particle in the presence of both an electric and magnetic field,

$$\mathcal{H} = -\vec{\mu} \cdot \vec{B} - \vec{d} \cdot \vec{E}. \tag{2.5}$$

The transformation properties of $\vec{E}$, $\vec{B}$, $\vec{\mu}$ and $\vec{d}$ are given in Table 2.2.3, and we see that while $\vec{\mu} \cdot \vec{B}$ is even under all three symmetries, $\vec{d} \cdot \vec{E}$ is odd under both P and T. Thus the existence of an EDM implies that both P and T are not good symmetries of the interaction Hamiltonian, Eq. (2.5). The EDM is a CP-odd quantity, and if observed, would be the manifestation of a new source of CP violation. The search for a muon EDM provides a unique opportunity to search for an EDM of a second-generation particle.

Table 2.1: Transformation properties of the magnetic and electric fields and dipole moments.

	$\vec{E}$	$\vec{B}$	$\vec{\mu}$ or $\vec{d}$
P	-	+	+
C	-	-	-
T	+	-	-

Concerning these symmetries, Ramsey states [30]:

> "However, it should be emphasized that while such arguments are appealing from the point of view of symmetry, they are not necessarily valid. Ultimately the validity of all such symmetry arguments must rest on experiment."

Fortunately this advice has been followed by many experimental investigators during the intervening 50 years. Since the Standard Model CP violation observed in the neutral kaon and B-meson systems is inadequate to explain the predominance of matter over antimatter in the universe, the search for new sources of CP violation beyond that embodied in the CKM formalism takes on a certain urgency. Searches for a permanent electric dipole moment of

the electron, neutron, and of an atomic nucleus have become an important part of the search for physics beyond the Standard Model. The present limits on subatomic EDMs is given in Table 2.2.3.

Table 2.2: EDM Limits for various systems

Particle	EDM Limit (e-cm)	SM value (e-cm)
p [31]	7.9×10^{-25}	
n [32]	2.9×10^{-26}	$\simeq 10^{-32}$
^{199}Hg [31]	3.1×10^{-29}	$\simeq 10^{-32}$
e^- [33]	1.05×10^{-27}	$< 10^{-41}$
μ [34]	1.8×10^{-19}	$< 10^{-38}$

2.3 Quick Summary of the Experimental Technique

Polarized muons are produced (see Chapter 7) and injected into the storage ring (see Chapter 12). The magnetic field is a dipole field, shimmed to ppm level uniformity. Vertical focusing is provided by electrostatic quadrupoles (see Chapter 13).

Two frequencies are measured experimentally: The rate at which the muon polarization turns relative to the momentum, called ω_a, and the value of the magnetic field normalized to the Larmor frequency of a free proton, ω_p.

The rate at which the spin[2] turns relative to the momentum, $\vec{\omega}_a = \vec{\omega}_S - \vec{\omega}_C$, where S and C stand for spin and cyclotron. These two frequencies are given by

$$\omega_S = -g\frac{Qe}{2m}B - (1-\gamma)\frac{Qe}{\gamma m}B; \tag{2.6}$$

$$\omega_C = -\frac{Qe}{m\gamma}B; \tag{2.7}$$

$$\omega_a = \omega_S - \omega_C = -\left(\frac{g-2}{2}\right)\frac{Qe}{m}B = -a\frac{Qe}{m}B \tag{2.8}$$

(where $e > 0$ and $Q = \pm 1$). There are two important features of ω_a: (i) It only depends on the anomaly rather than on the full magnetic moment; (ii) It depends linearly on the applied magnetic field. In the presence of an electric field ω_a is modified

$$\vec{\omega}_a = -\frac{Qe}{m}\left[a_\mu \vec{B} - \left(a_\mu - \left(\frac{mc}{p}\right)^2\right)\frac{\vec{\beta}\times\vec{E}}{c}\right] \tag{2.9}$$

If operated at the "magic" momentum $p_{magic} = m/\sqrt{a_\mu} \simeq 3.09$ GeV/c the electric field contribution cancels in first order, and requires a small correction in second order.

[2]The term 'spin' is often used in place of the more accurate term 'polarization'

The magnetic field is weighted by the muon distribution, and also averaged over the running time weighed by the number of stored muons to determine the value of ω_p which is combined with the average ω_a to determine a_μ. The reason for the use of these two frequencies, rather than B measured in tesla can be understood from Eq. 2.9. To obtain a_μ from this relationship requires precise knowledge of the muon charge to mass ratio.

To determine a_μ from the two frequencies ω_a and ω_p, we use the relationship

$$a_\mu = \frac{\omega_a/\omega_p}{\lambda_+ - \omega_a/\omega_p} = \frac{\mathcal{R}}{\lambda_+ - \mathcal{R}}\,, \tag{2.10}$$

where the ratio $\lambda_+ = \mu_{\mu^+}/\mu_p = 3.183\,345\,137\,(85)$ is the muon-to-proton magnetic moment ratio [43] measured from muonium (the μ^+e^- atom) hyperfine structure[45] (see Section 15.1.1 for futher details). Of course, to use λ_+ to determine a_{μ^-} requires the assumption of *CPT* invariance, *viz.* ($a_{\mu^+} = a_{\mu^-}$; $\lambda_+ = \lambda_-$). The comparison of $\mathcal{R}_{\mu^+}$ with $\mathcal{R}_{\mu^-}$ provides a *CPT* test. In E821

$$\Delta\mathcal{R} = \mathcal{R}_{\mu^-} - \mathcal{R}_{\mu^+} = (3.6 \pm 3.7) \times 10^{-9} \tag{2.11}$$

2.4 Results from E821

2.4.1 Measurement of a_μ

The E821 Collaboration working at the Brookhaven Laboratory AGS used an electric quadrupole field to provide vertical focusing in the storage ring, and shimmed the magnetic field to ± 1 ppm uniformity on average. The storage ring was operated at the "magic" momentum, $p_{magic} = 3.094$ GeV/c, ($\gamma_{magic} = 29.3$), such that $a_\mu = (m/p)^2$ and the electric field did not contribute to ω_a.[3] The result is [36, 37]

$$a_\mu^{\rm E821} = 116\,592\,089(54)_{stat}(33)_{syst}(63)_{tot} \times 10^{-11} \quad (\pm 0.54\,{\rm ppm}). \tag{2.12}$$

The results from E821 are shown in Fig. 2.1 (a) along with the Standard-Model value which is discussed below in Section 2.5. The importance of this result is illustrated in Fig. 2.1 (b) with a plot of the citations as a function of year.

2.5 The Standard-Model Value of a_μ

The Standard-Model (SM) value of the muon anomaly can be calculated with sub-parts-per-million precision[4]. The comparison between the measured and the SM prediction provides a test of the completeness of the Standard Model. At present, there appears to be a three- to four-standard deviation between these two values, which has motivated extensive theoretical and experimental work on the hadronic contributions to the muon anomaly.

A lepton ($\ell = e,\, \mu,\, \tau$) has a magnetic moment which is along its spin, given by the relationship

$$\vec{\mu}_\ell = g_\ell \frac{Qe}{2m_\ell}\vec{s}, \qquad \underbrace{g_\ell = 2}_{\rm Dirac}(1 + a_\ell), \qquad a_\ell = \frac{g_\ell - 2}{2} \tag{2.13}$$

[3] The magic momentum was first employed by the third CERN collaboration [25].

[4] This section is taken from Ref. [50]

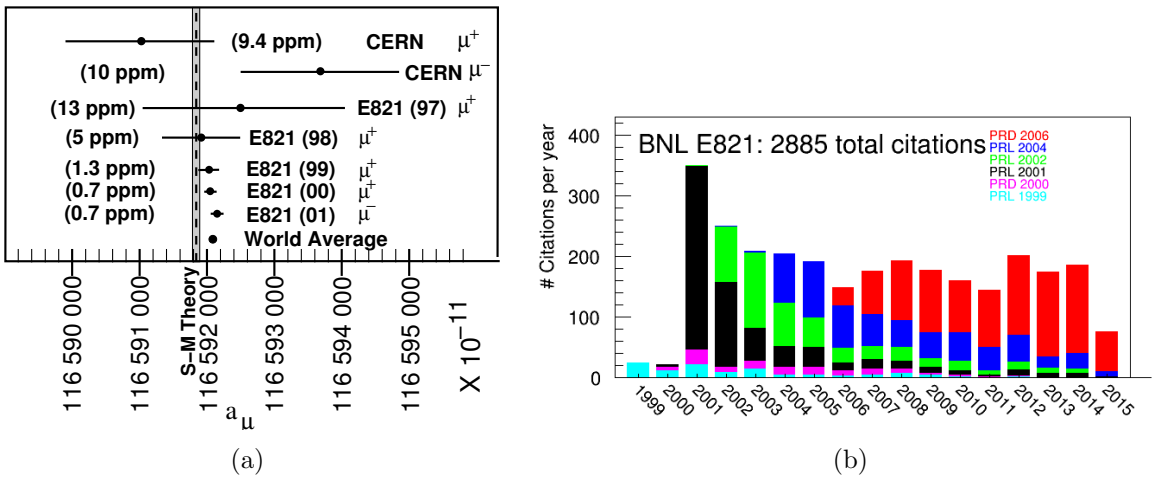

Figure 2.1: (a)Measurements of a_μ from CERN and BNL E821. The vertical band is the SM value using the hadronic contribution from Ref. [71] (see Table 2.3). (b) Citations to the E821 papers by year as of April 2015: light blue [38] plus [39]; green [40]; red [41]; blue [36]; and yellow the Physical Review article [37].

where $Q = \pm 1$, $e > 0$ and m_ℓ is the lepton mass. Dirac theory predicts that $g \equiv 2$, but experimentally, it is known to be greater than 2. The small number a, the anomaly, arises from quantum fluctuations, with the largest contribution coming from the mass-independent single-loop diagram in Fig. 2.2(a). With his famous calculation that obtained $a = (\alpha/2\pi) = 0.00116\cdots$, Schwinger [51] started an "industry", which required Aoyama, Hayakawa, Kinoshita and Nio to calculate more than 12,000 diagrams to evaluate the tenth-order (five loop) contribution [52].

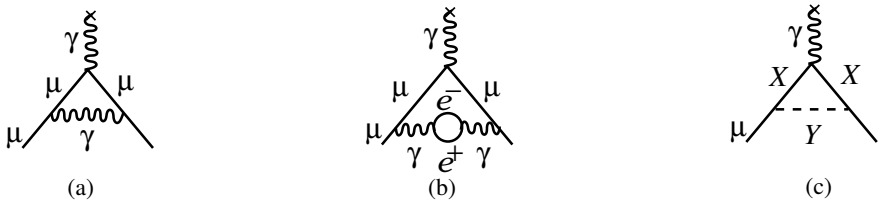

Figure 2.2: The Feynman graphs for: (a) The lowest-order (Schwinger) contribution to the lepton anomaly ; (b) The vacuum polarization contribution, which is one of five fourth-order, $(\alpha/\pi)^2$, terms; (c) The schematic contribution of new particles X and Y that couple to the muon.

The interaction shown in Fig. 2.2(a) is a chiral-changing, flavor-conserving process, which gives it a special sensitivity to possible new physics [53, 54]. Of course heavier particles can also contribute, as indicated by the diagram in Fig. 2.2(c). For example, $X = W^\pm$ and $Y = \nu_\mu$, along with $X = \mu$ and $Y = Z^0$, are the lowest-order weak contributions. In the Standard-Model, a_μ gets measureable contributions from QED, the strong interaction, and

from the electroweak interaction,

$$a^{SM} = a^{QED} + a^{Had} + a^{Weak}. \tag{2.14}$$

In this document we present the latest evaluations of the SM value of a_μ, and then discuss expected improvements that will become available over the next five to seven years. The uncertainty in this evaluation is dominated by the contribution of virtual hadrons in loops. A worldwide effort is under way to improve on these hadronic contributions. By the time that the Fermilab muon $(g-2)$ experiment, E989, reports a result later in this decade, the uncertainty should be significantly reduced. We emphasize that the existence of E821 at Brookhaven motivated significant work over the past thirty years that permitted more than an order of magnitude improvement in the knowledge of the hadronic contribution. Motivated by Fermilab E989 this work continues, and another factor of two improvement could be possible.

Both the electron [55] and muon [37] anomalies have been measured very precisely:

$$a_e^{exp} = 1\,159\,652\,180.73\,(28) \times 10^{-12} \quad \pm 0.24\,\text{ppb} \tag{2.15}$$

$$a_\mu^{exp} = 1\,165\,920\,89\,(63) \times 10^{-11} \quad \pm 0.54\,\text{ppm} \tag{2.16}$$

While the electron anomaly has been measured to $\simeq 0.3$ ppb (parts per billion) [55], it is significantly less sensitive to heavier physics, because the relative contribution of heavier virtual particles to the muon anomaly goes as $(m_\mu/m_e)^2 \simeq 43000$. Thus the lowest-order hadronic contribution to a_e is [56]: $a_e^{\text{had,LO}} = (1.875 \pm 0.017)\ 10^{-12}$, 1.5 ppb of a_e. For the muon the hadronic contribution is $\simeq 60$ ppm (parts per million). So with much less precision, when compared with the electron, the measured muon anomaly is sensitive to mass scales in the several hundred GeV region. This not only includes the contribution of the W and Z bosons, but perhaps contributions from new, as yet undiscovered, particles such as the supersymmetric partners of the electroweak gauge bosons (see Fig. 2.2(c)).

2.5.1 Summary of the Standard-Model Value of a_μ

QED Contribution

The QED contribution to a_μ is well understood. Recently the four-loop QED contribution has been updated and the full five-loop contribution has been calculated [52]. The present QED value is

$$a_\mu^{\text{QED}} = 116\ 584\ 718.951\ (0.009)(0.019)(0.007)(.077) \times 10^{-11} \tag{2.17}$$

where the uncertainties are from the lepton mass ratios, the eight-order term, the tenth-order term, and the value of α taken from the ^{87}Rb atom $\alpha^{-1}(Rb) = 137.035\,999\,049(90)$ [0.66 ppb]. [57].

Weak contributions

The electroweak contribution (shown in Fig. 2.3) is now calculated through two loops [58, 59, 60, 61, 62, 63, 64, 65]. The one loop result

$$\begin{aligned} a_\mu^{\mathrm{EW}(1)} &= \frac{G_F}{\sqrt{2}}\frac{m_\mu^2}{8\pi^2}\left\{ \underbrace{\frac{10}{3}}_{W} + \underbrace{\frac{1}{3}(1-4\sin^2\theta_W)^2 - \frac{5}{3}}_{Z} \right. \\ &+ \left. \mathcal{O}\left(\frac{m_\mu^2}{M_Z^2}\log\frac{M_Z^2}{m_\mu^2}\right) + \frac{m_\mu^2}{M_H^2}\int_0^1 dx \frac{2x^2(2-x)}{1-x+\frac{m_\mu^2}{M_H^2}x^2} \right\} \\ &= 194.8 \times 10^{-11}\,, \end{aligned} \tag{2.18}$$

was calculated by five separate groups [66] shortly after the Glashow-Salam-Weinberg theory was shown by 't Hooft to be renormalizable. Due to the small Yukawa coupling of the Higgs boson to the muon, only the W and Z bosons contribute at a measurable level in the lowest-order electroweak term.

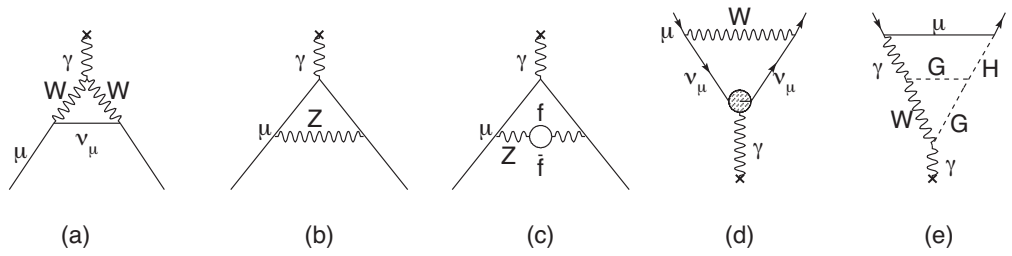

Figure 2.3: Weak contributions to the muon anomalous magnetic moment. Single-loop contributions from (a) virtual W and (b) virtual Z gauge bosons. These two contributions enter with opposite sign, and there is a partial cancellation. The two-loop contributions fall into three categories: (c) fermionic loops which involve the coupling of the gauge bosons to quarks, (d) bosonic loops which appear as corrections to the one-loop diagrams, and (e) a new class of diagrams involving the Higgs where G is the longitudinal component of the gauge bosons. See Ref. [67] for details. The $\times$ indicates the photon from the magnetic field.

The two-loop electroweak contribution (see Figs. 2.3(c-e)), which is negative [60, 59, 58], has been re-evaluated using the LHC value of the Higgs mass and consistently combining exact two-loop with leading three-loop results [65]. The total electroweak contribution is

$$a_\mu^{\mathrm{EW}} = (153.6 \pm 1.0) \times 10^{-11} \tag{2.19}$$

where the error comes from hadronic effects in the second-order electroweak diagrams with quark triangle loops, along with unknown three-loop contributions [61, 68, 69, 70]. The leading logs for the next-order term have been shown to be small [61, 65]. The weak contribution is about 1.3 ppm of the anomaly, so the experimental uncertainty on a_μ of ± 0.54 ppm now probes the weak scale of the Standard Model.

Hadronic contribution

The hadronic contribution to a_μ is about 60 ppm of the total value. The lowest-order diagram shown in Fig. 2.4(a) dominates this contribution and its error, but the hadronic light-by-light contribution Fig. 2.4(e) is also important. We discuss both of these contributions below.

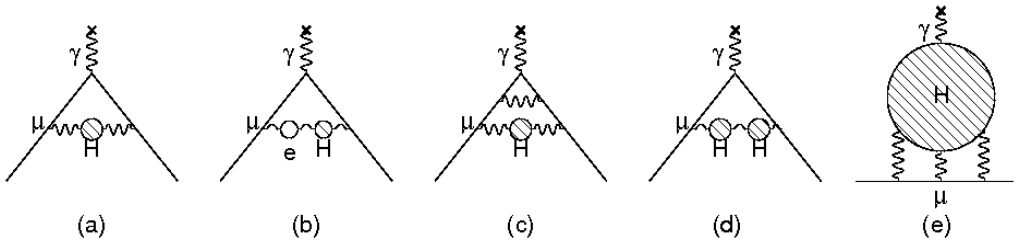

Figure 2.4: The hadronic contribution to the muon anomaly, where the dominant contribution comes from the lowest-order diagram (a). The hadronic light-by-light contribution is shown in (e).

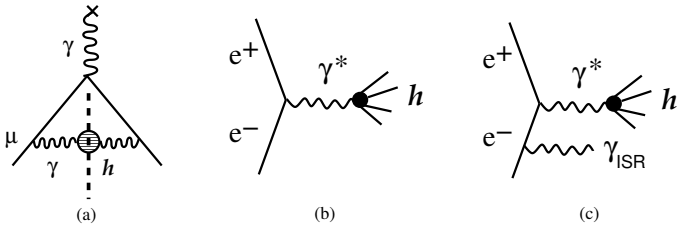

Figure 2.5: (a) The "cut" hadronic vacuum polarization diagram; (b) The e^+e^- annihilation into hadrons; (c) Initial state radiation accompanied by the production of hadrons.

The energy scale for the virtual hadrons is of order $m_\mu c^2$, well below the perturbative region of QCD. However it can be calculated from the dispersion relation shown pictorially in Fig. 2.5,

$$a_\mu^{\mathrm{had;LO}} = \left(\frac{\alpha m_\mu}{3\pi}\right)^2 \int_{m_\pi^2}^{\infty} \frac{ds}{s^2} K(s) R(s), \quad \text{where} \quad R \equiv \frac{\sigma_{\mathrm{tot}}(e^+e^- \to \text{hadrons})}{\sigma(e^+e^- \to \mu^+\mu^-)}\,, \tag{2.20}$$

using the measured cross sections for $e^+e^- \to$ hadrons as input, where $K(s)$ is a kinematic factor ranging from 0.4 at $s = m_\pi^2$ to 0 at $s = \infty$ (see Ref. [67]). This dispersion relation relates the bare cross section for e^+e^- annihilation into hadrons to the hadronic vacuum polarization contribution to a_μ. Because the integrand contains a factor of s^{-2}, the values of $R(s)$ at low energies (the ρ resonance) dominate the determination of $a_\mu^{\mathrm{had;LO}}$, however at the level of precision needed, the data up to 2 GeV are very important. This is shown in Fig. 2.6, where the left-hand chart gives the relative contribution to the integral for the different energy regions, and the right-hand gives the contribution to the error squared on the integral. The contribution is dominated by the two-pion final state, but other low-energy

multi-hadron cross sections are also important. These data for e^+e^- annihilation to hadrons are also important as input into the determination of $\alpha_{QED}(M_Z)$ and other electroweak precision measurements.

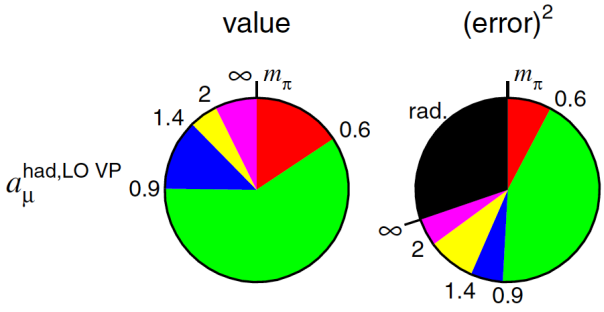

Figure 2.6: Contributions to the dispersion integral for different energy regions, and to the associated error (squared) on the dispersion integral in that energy region. Taken from Hagiwara et al. [72].

Two recent analyses [71, 72] using the $e^+e^- \to hadrons$ data obtained:

$$a_\mu^{\text{had;LO}} = (6\ 923 \pm 42) \times 10^{-11}\,, \tag{2.21}$$

$$a_\mu^{\text{had;LO}} = (6\ 949 \pm 43) \times 10^{-11}\,, \tag{2.22}$$

respectively. Important earlier global analyses include those of Hagiwara et al. [73], Davier, et al., [74], Jegerlehner and Nyffler [75].

In the past, hadronic τ spectral functions and CVC, together with isospin breaking corrections have been used to calculate the hadronic contribution [76, 71]. While the original predictions showed a discrepancy between e^+e^- and τ based evaluations, it has been shown that after γ-ρ mixing is taken into account, the two are compatible [77]. Recent evaluations based on a combined e^+e^- and τ data fit using the Hidden Local Symmetry (HLS) model have come to similar conclusions and result in values for a_μ^{HVP} that are smaller than the direct evaluation without the HLS fit [78, 79].

The most recent evaluation of the next-to-leading order hadronic contribution shown in Fig. 2.4(b-d), which can also be determined from a dispersion relation, is [72]

$$a_\mu^{\text{had;NLO}} = (-98.4 \pm 0.6_{\text{exp}} \pm 0.4_{\text{rad}}\ ) \times 10^{-11}\,. \tag{2.23}$$

Very recently, also the next-to-next-to-leading order hadronic contribution has been evaluated [80], with a result of the order of the expected future experimental uncertainty. This result will be included in future evaluations of the full SM theory prediction.

Hadronic light-by-light contribution

The hadronic light-by-light contribution (HLbL) cannot at present be determined from data, but rather must be calculated using hadronic models that correctly reproduce properties

of QCD. This contribution is shown below in Fig. 2.7(a). It is dominated by the long-distance contribution shown in Fig. 2.7(b). In fact, in the so called chiral limit where the mass gap between the pseudoscalars (Goldstone-like) particles and the other hadronic particles (the ρ being the lowest vector state in Nature) is considered to be large, and to leading order in the $1/N_c$–expansion (N_c the number of colors), this contribution has been calculated analytically [81] and provides a long-distance constraint to model calculations. There is also a short-distance constraint from the operator product expansion (OPE) of two electromagnetic currents which, in specific kinematic conditions, relates the light-by-light scattering amplitude to an Axial-Vector-Vector triangle amplitude for which one has a good theoretical understanding [82].

Unfortunately, the two asymptotic QCD constraints mentioned above are not sufficient for a full model independent evaluation of the HLbL contribution. Most of the last decade calculations found in the literature are compatible with the QCD chiral and large-N_c limits. They all incorporate the π^0-exchange contribution modulated by $\pi^0\gamma^*\gamma^*$ form factors correctly normalized to the Adler, Bell-Jackiw point-like coupling. They differ, however, on whether or not they satisfy the particular OPE constraint mentioned above, and in the shape of the vertex form factors which follow from the different models.

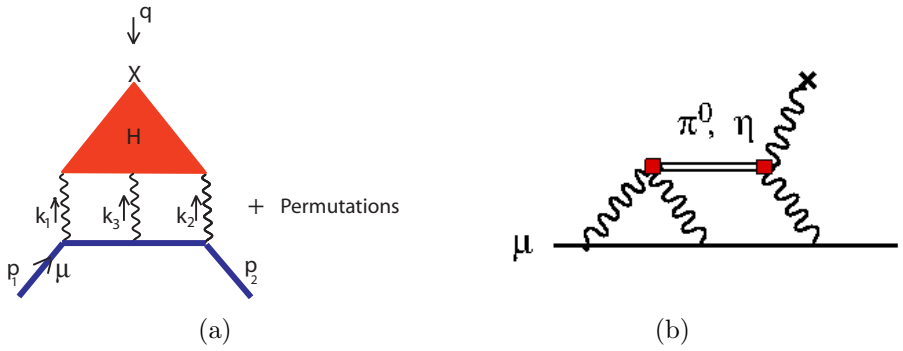

Figure 2.7: (a)The Hadronic Light-by contribution. (b) The pseudoscalar meson contribution.

A synthesis of the model contributions, which was agreed to by authors from each of the leading groups that have been working in this field, can be found in ref. [83][5]. They obtained

$$a_\mu^{\rm HLbL} = (105 \pm 26) \times 10^{-11} \,. \tag{2.24}$$

An alternate evaluation [75, 84] obtained, $a_\mu^{\rm HLbL} = (116 \pm 40) \times 10^{-11}$, which agrees well with the Glasgow Consensus [83]. Additional work on this contribution is underway on a number of fronts, including on the lattice. A workshop was held in March 2011 at the Institute for Nuclear Theory in Seattle [85] which brought together almost all of the interested experts. A second workshop followed at the Mainz Institute for Theoretical Physics in April 2014 [86].

[5]This compilation is generally referred to as the "Glasgow Consensus" since it grew out of a workshop in Glasgow in 2007. http://www.ippp.dur.ac.uk/old/MuonMDM/

One important point should be stressed here. The main physics of the hadronic light-by-light scattering contribution is well understood. In fact, but for the sign error unraveled in 2002, the theoretical predictions for $a_\mu^{\rm HLbL}$ have been relatively stable for more than ten years[6].

2.5.2 Summary of the Standard-Model Value and Comparison with Experiment

We determine the SM value using the new QED calculation from Aoyama [52]; the electroweak from Ref. [65], the hadronic light-by-light contribution from the "Glasgow Consensus" [83]; and lowest-order hadronic contribution from Davier, et al., [71], or Hagiwara et al., [72], and the higher-order hadronic contribution from Ref. [72]. A summary of these values is given in Table 2.3.

Table 2.3: Summary of the Standard-Model contributions to the muon anomaly. Two values are quoted because of the two recent evaluations of the lowest-order hadronic vacuum polarization.

	VALUE ($\times 10^{-11}$) UNITS
QED ($\gamma + \ell$)	$116\,584\,718.951 \pm 0.009 \pm 0.019 \pm 0.007 \pm 0.077_\alpha$
HVP(lo) [71]	$6\,923 \pm 42$
HVP(lo) [72]	$6\,949 \pm 43$
HVP(ho) [72]	-98.4 ± 0.7
HLbL	105 ± 26
EW	153.6 ± 1.0
Total SM [71]	$116\,591\,802 \pm 42_{\text{H-LO}} \pm 26_{\text{H-HO}} \pm 2_{\text{other}}\,(\pm 49_{\text{tot}})$
Total SM [72]	$116\,591\,828 \pm 43_{\text{H-LO}} \pm 26_{\text{H-HO}} \pm 2_{\text{other}}\,(\pm 50_{\text{tot}})$

This SM value is to be compared with the combined a_μ^+ and a_μ^- values from E821 [37] corrected for the revised value of $\lambda = \mu_\mu/\mu_p$ from Ref [43],

$$a_\mu^{\rm E821} = (116\,592\,089 \pm 63) \times 10^{-11} \quad (0.54\,\text{ppm}), \tag{2.25}$$

which give a difference of

$$\Delta a_\mu(\text{E821} - \text{SM}) = (287 \pm 80) \times 10^{-11}\ [71] \tag{2.26}$$

$$= (261 \pm 80) \times 10^{-11}\ [72] \tag{2.27}$$

depending on which evaluation of the lowest-order hadronic contribution that is used [71, 72].

This comparison between the experimental values and the present Standard-Model value is shown graphically in Fig. 2.1. The lowest-order hadronic evaluation of Ref. [79] using the

[6] A calculation using a Dyson-Schwinger approach [87] initially reported a much larger value for the HLbL contribution. Subsequently a numerical mistake was found. These authors are continuing this work, but the calculation is still incomplete.

hidden local symmetry model results in a difference between experiment and theory that ranges between 4.1 to 4.7σ.

This difference of 3.3 to 3.6 standard deviations is tantalizing, but we emphasize that whatever the final agreement between the measured and SM value turns out to be, it will have significant implications on the interpretation of new phenomena that might be found at the LHC and elsewhere. Because of the power of a_μ to constrain, or point to, speculative models of New Physics, the E821 results have been highly cited, see Fig. 2.1 (b) and Section 2.7 below.

2.6 Expected Improvements in the Standard-Model Value

The present uncertainty on the theoretical value is dominated by the hadronic contributions [71, 72] (see Table 2.3). The lowest-order contribution determined from $e^+e^- \to$ hadrons data using a dispersion relation is theoretically relatively straightforward. It does require the combination of data sets from different experiments. The only significant theoretical uncertainty comes from radiative corrections, such as vacuum polarization (running α), along with initial and final state radiation effects, which are needed to obtain the correct hadronic cross section at the required level of precision. This was a problem for the older data sets. In the analysis of the data collected over the past 15 years, which now dominate the determination of the hadronic contribution, the treatment of radiative corrections has been significantly improved. Nevertheless, an additional uncertainty due to the treatment of these radiative corrections in the older data sets has been estimated to be of the order of 20×10^{-11} [72]. As more data become available, this uncertainty will be significantly reduced.

There are two methods that have been used to measure the hadronic cross sections: The energy scan (see Fig. 2.5(b)), and using initial state radiation with a fixed beam energy to measure the cross section for energies below the total center-of-mass energy of the colliding beams (see Fig. 2.5(c)). Both are being employed in the next round of measurements. The data from the new experiments that are now underway at VEPP-2000 in Novosibirsk and BESIII in Beijing, when combined with the analysis of existing multi-hadron final-state data from BaBar and Belle, should significantly reduce the uncertainty on the lowest-order hadronic contribution.

The hadronic-light-by-light contribution does not lend itself easily to determination by a dispersion relation, see however recent progress reported in Ref. [88] and in talks at the Mainz workshop [86]. Nevertheless there are some experimental data that can help to pin down related amplitudes and to constrain form factors used in the model calculations.

2.6.1 Lowest-order Hadronic Contribution

Much experimental and theoretical work is going on worldwide to refine the hadronic contribution. The theory of $(g-2)$, relevant experiments to determine the hadronic contribution, including work on the lattice, have featured prominently in the series of tau-lepton workshops and PHIPSI workshops which are held in alternate years. Over the development

period of Fermilab E989, we expect further improvements in the SM-theory evaluation. This projection is based on the following developments:

Novosibirsk

The VEPP2M machine has been upgraded to VEPP-2000. The maximum energy has been increased from $\sqrt{s} = 1.4$ GeV to 2.0 GeV. Additionally, the SND detector has been upgraded and the CMD2 detector was replaced by the much-improved CMD3 detector. The cross section will be measured from threshold to 2.0 GeV using an energy scan, filling in the energy region between 1.4 GeV, where the previous scan ended, up to 2.0 GeV, the lowest energy point reached by the BES collaboration in their measurements. See Fig. 2.6 for the present contribution to the overall error from this region. Engineering runs began in 2009, and data collection started in 2011. So far two independent energy scans between 1.0 and 2.0 GeV were performed in 2011 and 2012. The peak luminosity of $3 \times 10^{31}\text{cm}^{-2}\text{s}^{-1}$ was achieved, which was limited by the positron production rate. The new injection facility, scheduled to be commissioned during the 2013-2014 upgrade, should permit the luminosity to reach $10^{32}\text{cm}^{-2}\text{s}^{-1}$. Data collection resumed in late 2012 with a new energy scan over energies below 1.0 GeV. The goal of experiments at VEPP-2000 is to achieve a systematic error 0.3-0.5% in the $\pi^+\pi^-$ channel, with negligible statistical error in the integral. The high statistics, expected at VEPP-2000, should allow a detailed comparison of the measured cross-sections with ISR results at BaBar and DAΦNE. After the upgrade, experiments at VEPP-2000 plan to take a large amount of data at 1.8-2 GeV, around the $N\bar{N}$ threshold. This will permit ISR data with the beam energy of 2 GeV, which is between the PEP2 energy at the $\Upsilon(4S)$ and the 1 GeV ϕ energy at the DAΦNE facility in Frascati. The dual ISR and scan approach will provide an important cross check on the two central methods used to determine the HVP.

The BESIII Experiment

The BESIII experiment at the Beijing tau-charm factory BEPC-II has already collected several inverse femtobarns of integrated luminosity at various centre-of-mass energies in the range 3 - 4.5 GeV. The ISR program includes cross section measurements of: $e^+e^- \to \pi^+\pi^-$, $e^+e^- \to \pi^+\pi^-\pi^0$, $e^+e^- \to \pi^+\pi^-\pi^0\pi^0$ – the final states most relevant to $(g-2)_\mu$. Presently, a data sample of 2.9 fb^{-1} at $\sqrt{s} = 3.77$ GeV is being analyzed, but new data at $\sqrt{s} > 4$ GeV can be used for ISR physics as well and will double the statistics. Using these data, hadronic invariant masses from threshold up to approximately 3.5 GeV can be accessed at BESIII. Although the integrated luminosities are orders of magnitude lower compared to the B-factory experiments BaBar and BELLE, the ISR method at BESIII still provides competitive statistics. This is due to the fact that the most interesting mass range for the HVP contribution of $(g-2)_\mu$, which is below approximately 3 GeV, is very close to the centre-of-mass energy of the collider BEPC-II and hence leads to a configuration where only relatively low-energetic ISR photons need to be emitted, providing a high ISR cross section. Furthermore, in contrast to the B factories, small angle ISR photons can be included in the event selection for kinematic reasons which leads to a very high overall geometrical acceptance. Compared to the KLOE experiment, background from final state radiation

(FSR) is reduced significantly as this background decreases with increasing center of mass energies of the collider. BESIII is aiming for a precision measurement of the ISR R-ratio $R_{\rm ISR} = N(\pi\pi\gamma)/N(\mu\mu\gamma)$ with a precision of about 1%. This requires an excellent pion-muon separation, which is achieved by training a multi-variate neural network. As a preliminary result, an absolute cross section measurement of the reaction $e^+e^- \to \mu^+\mu^-\gamma$ has been achieved, which agrees with the QED prediction within 1% precision.

Moreover, at BESIII a new energy scan campaign is planned to measure the inclusive R ratio in the energy range between 2.0 and 4.6 GeV. Thanks to the good performance of the BEPC-II accelerator and the BESIII detector a significant improvement upon the existing BESII measurement can be expected. The goal is to arrive at an inclusive R ratio measurement with about 1% statistical and 3% systematic precision per scan point.

Summary of the Lowest-Order Improvements from Data

A substantial amount of new e^+e^- cross section data will become available over the next few years. These data have the potential to significantly reduce the error on the lowest-order hadronic contribution. These improvements can be obtained by reducing the uncertainties of the hadronic cross-sections from 0.7% to 0.4% in the region below 1 GeV and from 6% to 2% in the region between 1 and 2 GeV as shown in Table 2.4.

	$\delta(\sigma)/\sigma$ present	δa_μpresent	$\delta(\sigma)/\sigma$ future	δa_μfuture
$\sqrt{s} < 1$ GeV	0.7%	33	0.4%	19
$1 < \sqrt{s} < 2$ GeV	6%	39	2%	13
$\sqrt{s} > 2$ GeV		12		12
total		53		26

Table 2.4: Overall uncertainty of the cross-section measurement required to get the reduction of uncertainty on a_μ in units 10^{-11} for three regions of $\sqrt{s}$ (from Ref. [93]).

Lattice calculation of the Lowest-Order HVP:

With computer power presently available, it is possible for lattice QCD calculations to make important contributions to our knowledge of the lowest-order hadronic contribution. Using several different discretizations for QCD, lattice groups around the world are computing the HVP [94, 95, 96, 97, 98] (see also several recent talks at Lattice 2013 (Mainz)). The varied techniques have different systematic errors, but in the continuum limit $a \to 0$ they should all agree. Many independent calculations provide a powerful check on the lattice results, and ultimately the dispersive ones too.

Several groups are now performing simulations with physical light quark masses on large boxes, eliminating significant systematic errors. So called quark-disconnected diagrams are also being calculated, and several recent theory advances will help to reduce systematic errors associated with fitting and the small q^2 regime [99, 95, 100, 101, 102, 103]. While the HVP systematic errors are well understood, significant computational resources are needed

to control them at the $\sim 1\%$ level, or better. Taking into account current resources and those expected in the next few years, the lattice-QCD uncertainty on a_μ(HVP), currently at the $\sim 5\%$-level, can be reduced to 1 or 2% within the next few years. This is already interesting as a wholly independent check of the dispersive results for a_μ(HVP). With increasing experience and computer power, it should be possible to compete with the e^+e^- determination of a_μ(HVP) by the end of the decade, perhaps sooner with additional technical advances.

2.6.2 The Hadronic Light-by-Light contribution

There are two major approaches to improving the HLbL contribution, beyond theoretical work on refining the existing model calculations: Using experimental data from measurements of γ^* physics at BESIII and KLOE; calculations on the lattice.

Any experimental information on the neutral pion lifetime and the transition form factor is important in order to constrain the models used for calculating the pion-exchange contribution (see Fig. 2.7(b)). However, having a good description, e.g. for the transition form factor, is only necessary, not sufficient, in order to uniquely determine $a_\mu^{\mathrm{HLbL};\pi^0}$. As stressed in Ref. [106], what enters in the calculation of $a_\mu^{\mathrm{HLbL};\pi^0}$ is the fully off-shell form factor $\mathcal{F}_{\pi^{0*}\gamma^*\gamma^*}((q_1+q_2)^2, q_1^2, q_2^2)$ (vertex function), where also the pion is off-shell with 4-momentum (q_1+q_2). Such a (model dependent) form factor can for instance be defined via the QCD Green's function $\langle VVP\rangle$, see Ref. [84] for details. The form factor with on-shell pions is then given by $\mathcal{F}_{\pi^0\gamma^*\gamma^*}(q_1^2, q_2^2) \equiv \mathcal{F}_{\pi^{0*}\gamma^*\gamma^*}(m_\pi^2, q_1^2, q_2^2)$. Measurements of the transition form factor $\mathcal{F}_{\pi^0\gamma^*\gamma}(Q^2) \equiv \mathcal{F}_{\pi^{0*}\gamma^*\gamma^*}(m_\pi^2, -Q^2, 0)$ are in general only sensitive to a subset of the model parameters and do not permit the reconstruction the full off-shell form factor.

For different models, the effects of the off-shell pion can vary a lot. In Ref. [84] the off-shell lowest meson dominance (LMD) plus vector meson dominance (LMD+V) form factor was proposed and the estimate $a_{\mu;\mathrm{LMD+V}}^{\mathrm{HLbL};\pi^0} = (72 \pm 12) \times 10^{-11}$ was obtained (see also Ref. [107]). The error estimate comes from the variation of all model parameters, where the uncertainty of the parameters related to the off-shellness of the pion completely dominates the total error. In contrast to the off-shell LMD+V model, many other models, e.g. the VMD model or constituent quark models, do not have these additional sources of uncertainty related to the off-shellness of the pion. These models often have only very few parameters, which can all be fixed by measurements of the transition form factor or from other observables. Therefore, for such models, the precision of the KLOE-2 measurement can dominate the total precision of $a_\mu^{\mathrm{HLbL};\pi^0}$.

Essentially all evaluations of the pion-exchange contribution use for the normalization of the form factor, $\mathcal{F}_{\pi^{0*}\gamma^*\gamma^*}(m_\pi^2, 0, 0) = 1/(4\pi^2 F_\pi)$, as derived from the Wess-Zumino-Witten (WZW) term. Then the value $F_\pi = 92.4$ MeV is used without any error attached to it, i.e. a value close to $F_\pi = (92.2 \pm 0.14)$ MeV, obtained from $\pi^+ \to \mu^+\nu_\mu(\gamma)$ [108]. If one uses the decay width $\Gamma_{\pi^0\to\gamma\gamma}$ for the normalization of the form factor, an additional source of uncertainty enters, which has not been taken into account in most evaluations [109]. Until recently, the experimental world average of $\Gamma_{\pi^0\to\gamma\gamma}^{PDG} = 7.74 \pm 0.48$ eV [108] was only known to 6.2% precision. Due to the poor agreement between the existing data, the PDG error of the width average is inflated (scale factor of 2.6) and it gives an additional motivation for new precise measurements. The PrimEx Collaboration, using a Primakoff effect experiment

at JLab, has achieved 2.8% fractional precision [110]. There are plans to further reduce the uncertainty to the percent level. Though theory and experiment are in a fair agreement, a better experimental precision is needed to really test the theory predictions.

Impact of KLOE-2 measurements on $a_\mu^{\mathrm{HLbL};\pi^0}$

For the new data taking of the KLOE-2 detector, which is expected to start by the end of 2013, new small angle tagging detectors have been installed along DAΦNE beam line.

These "High Energy Tagger" detectors [111] offer the possibility to study a program of $\gamma\gamma$ physics through the process $e^+e^- \to e^+\gamma^* e^-\gamma^* \to e^+e^- X$.

Thus a coincidence between the scattered electrons and a π^0 would provide information on $\gamma^*\gamma^* \to \pi^0$ [104], and will provide experimental constraints on the models used to calculate the hadronic light-by-light contribution [105].

In Ref. [112] it was shown that planned measurements at KLOE-2 could determine the $\pi^0 \to \gamma\gamma$ decay width to 1% statistical precision and the $\gamma^*\gamma \to \pi^0$ transition form factor $\mathcal{F}_{\pi^0\gamma^*\gamma}(Q^2)$ for small space-like momenta, 0.01 GeV$^2 \leq Q^2 \leq$ 0.1 GeV^2, to 6% statistical precision in each bin. The simulations have been performed with the Monte-Carlo program EKHARA [113] for the process $e^+e^- \to e^+e^-\gamma^*\gamma^* \to e^+e^-\pi^0$, followed by the decay $\pi^0 \to \gamma\gamma$ and combined with a detailed detector simulation. The results of the simulations are shown in Figure 2.8. The KLOE-2 measurements will allow to almost directly measure the slope of the form factor at the origin and check the consistency of models which have been used to extrapolate the data from larger values of Q^2 down to the origin. With the decay width $\Gamma^{\mathrm{PDG}}_{\pi^0\to\gamma\gamma}$ [$\Gamma^{\mathrm{PrimEx}}_{\pi^0\to\gamma\gamma}$] and current data for the transition form factor $\mathcal{F}_{\pi^0\gamma^*\gamma}(Q^2)$, the error on $a_\mu^{\mathrm{HLbL};\pi^0}$ is $\pm 4 \times 10^{-11}$ [$\pm 2 \times 10^{-11}$], not taking into account the uncertainty related to the off-shellness of the pion. Including the simulated KLOE-2 data reduces the error to $\pm(0.7 - 1.1) \times 10^{-11}$.

BESIII Hadronic light-by-light contribution

Presently, data taken at $\sqrt{s}$ =3.77 GeV are being analyzed to measure the form factors of the reactions $\gamma^*\gamma \to X$, where $X = \pi^0, \eta, \eta', 2\pi$.

BESIII has launched a program of two-photon interactions with the primary goal to measure the transition form factors (TFF) of pseudoscalar mesons as well as of the two-pion system in the spacelike domain. These measurements are carried out in the single-tag mode, i.e. by tagging one of the two beam leptons at large polar angles and by requiring that the second lepton is scattered at small polar angles. With these kinematics the form factor, which in general depends on the virtualities of the two photons, reduces to $F(Q^2)$, where Q^2 is the negative momentum transfer of the tagged lepton. At BESIII, the process $\gamma\gamma^* \to \pi^0$, which is known to play a leading contribution in the HLbL correction to $(g-2)$, can be measured with unprecedented precision in the Q^2 range between 0.3 GeV^2 and 4 GeV^2. In the future BESIII will also embark on untagged as well as double-tag measurements, in which either both photons are quasi-real or feature a high virtuality. The goal is to carry out this program for the final states $\pi^0, \eta, \eta', \pi\pi$. It still needs to be proven that the small angle detector, which recently has been installed close to the BESIII beamline, can be used for the two-photon program.

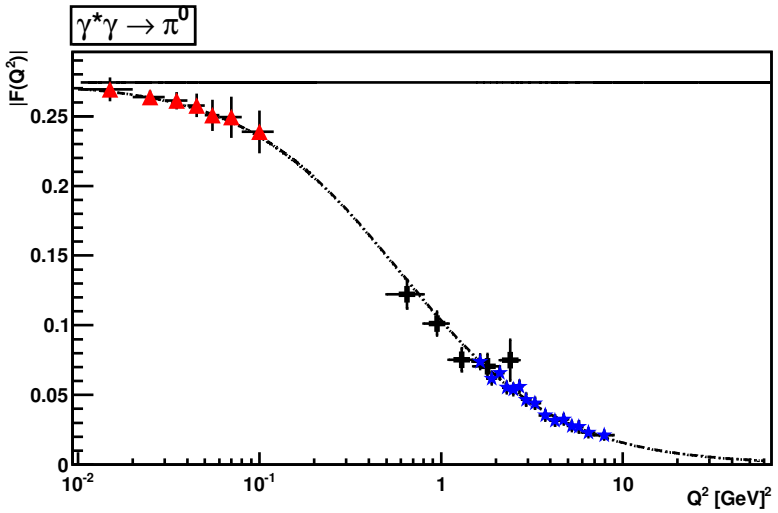

Figure 2.8: Simulation of KLOE-2 measurement of $F(Q^2)$ (red triangles) with statistical errors for 5 fb^{-1}, corresponding to one year of data taking. The dashed line is the $F(Q^2)$ form factor according to the LMD+V model [84, 107], the solid line is $F(0) = 1/(4\pi^2 F_\pi)$ given by the Wess-Zumino-Witten term. Data [114] from CELLO (black crosses) and CLEO (blue stars) at high Q^2 are also shown for illustration.

Lattice calculation of Hadronic Light-by-Light Scattering:

Model calculations show that the hadronic light-by-light (HLbL) contribution is roughly $(105 \pm 26) \times 10^{-11}$, ~ 1 ppm of a_μ. Since the error attributed to this estimate is difficult to reduce, a modest, but first principles calculation on the lattice would have a large impact. Recent progress towards this goal has been reported [96], where a non-zero signal (statistically speaking) for a part of the amplitude emerged in the same ball-park as the model estimate. The result was computed at non-physical quark mass, with other systematic errors mostly uncontrolled. Work on this method, which treats both QED and QCD interactions non-perturbatively, is continuing. The next step is to repeat the calculation on an ensemble of gauge configurations that has been generated with electrically charged sea quarks (see the poster by Blum presented at Lattice 2013). The charged sea quarks automatically include the quark disconnected diagrams that were omitted in the original calculation and yield the complete amplitude. As for the HVP, the computation of the HLbL contribution requires significant resources which are becoming available. While only one group has so far attempted the calculation, given the recent interest in the HVP contribution computed in lattice QCD and electromagnetic corrections to hadronic observables in general, it seems likely that others will soon enter the game. And while the ultimate goal is to compute the HLbL contribution to 10% accuracy, or better, we emphasize that a lattice calculation with even a solid 30% error would already be very interesting. Such a result, while not guaranteed, is not out of the question during the next 3-5 years.

2.6.3 Summary of the Standard Model Contribution

The muon and electron anomalous magnetic moments are among, if not the most precisely measured and calculated quantities in all of physics. The theoretical uncertainty on the Standard-Model contribution to a_μ is $\simeq 0.4$ ppm, slightly smaller than the experimental error from BNL821. The new Fermilab experiment, E989, will achieve a precision of 0.14 ppm. While the hadronic corrections will most likely not reach that level of precision, their uncertainty will be significantly decreased. The lowest-order contribution will be improved by new data from Novosibirsk and BESIII. On the timescale of the first results from E989, the lattice will also become relevant.

The hadronic light-by-light contribution will also see significant improvement. The measurements at Frascati and at BESIII will provide valuable experimental input to constrain the model calculations. There is hope that the lattice could produce a meaningful result by 2018.

We summarize possible near-future improvements in the table below. Since it is difficult to project the improvements in the hadronic light-by-light contribution, we assume a conservative improvement: That the large amount of work that is underway to understand this contribution, both experimentally and on the lattice, will support the level of uncertainty assigned in the "Glasgow Consensus". With these improvements, the overall uncertainty on Δa_μ could be reduced by a factor 2. In case the central value would remain the same, the statistical significance would become 7-8 standard deviations, as it can be seen in Fig. 2.9.

Error	[71]	[72]	Future
$\delta a_\mu^{\rm SM}$	49	50	35
$\delta a_\mu^{\rm HLO}$	42	43	26
$\delta a_\mu^{\rm HLbL}$	26	26	25
$\delta(a_\mu^{\rm EXP} - a_\mu^{\rm SM})$	80	80	40

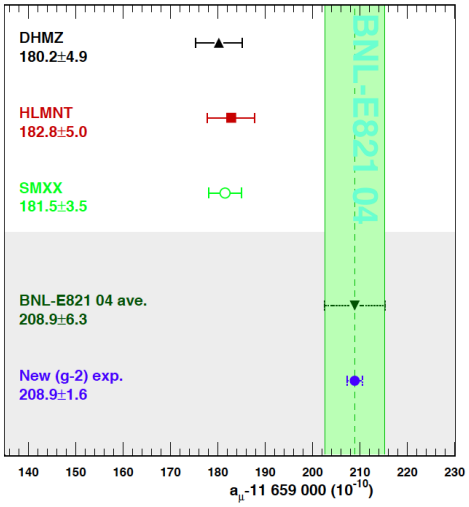

Figure 2.9: Estimated uncertainties δa_μ in units of 10^{-11} according to Refs. [71, 72] and (last column) prospects for improved precision in the e^+e^- hadronic cross-section measurements. The final row projects the uncertainty on the difference with the Standard Model, Δa_μ. The figure give the comparison between $a_\mu^{\rm SM}$ and $a_\mu^{\rm EXP}$. DHMZ is Ref. [71], HLMNT is Ref. [72]; "SMXX" is the same central value with a reduced error as expected by the improvement on the hadronic cross section measurement (see text); "BNL-E821 04 ave." is the current experimental value of a_μ; "New (g-2) exp." is the same central value with a fourfold improved precision as planned by the future (g-2) experiments at Fermilab and J-PARC.

Thus the prognosis is excellent that the results from E989 will clarify whether the measured value of a_μ contains contributions from outside of the Standard Model. Even if there is no improvement on the hadronic error, but the central theory and experimental values remain the same, the significance of the difference would be over 5σ. However, with the worldwide effort to improve on the Standard-Model value, it is most likely that the comparison will be even more convincing.

2.7 Physics Beyond the Standard Model

For many years, the muon anomaly has played an important role in constraining physics beyond the SM [47, 48, 53, 115, 54, 116]. The more than 2000 citations to the major E821 papers [37, 36, 41, 40], demonstrates that this role continues. The citations are shown as a function of year in Fig. 2.1 (b). It is apparent that with the LHC results available in 2012, interest in the BNL results has risen significantly. As discussed in the previous section, the present SM value is smaller than the experimental value by $\Delta a_\mu(\text{E821} - \text{SM})$. The discrepancy depends on the SM evaluation, but it is generally in the $> 3\sigma$ region; a representative value is $(261 \pm 80) \times 10^{-11}$, see Eq. (2.27).

In this section, we discuss how the muon anomaly provides a unique window to search for physics beyond the standard model. If such new physics is discovered elsewhere, e.g. at the LHC, then a_μ will play an important role in sorting out the interpretation of those discoveries. We discuss examples of constraints placed on various models that have been proposed as extensions of the standard model. Perhaps the ultimate value of an improved limit on a_μ will come from its ability to constrain the models that have not yet been invented.

Varieties of physics beyond the Standard Model

The LHC era has had its first spectacular success in summer 2012 with the discovery of a new particle compatible with the standard model Higgs boson. With more data, the LHC experiments will continue to shed more light on the nature of electroweak symmetry breaking (EWSB). It is very likely that EWSB is related to new particles, new interactions, or maybe to new concepts such as supersymmetry, extra dimensions, or compositeness. Further open questions in particle physics, related e.g. to the nature of dark matter, the origin of flavor or grand unification, indicate that at or even below the TeV scale there could be rich physics beyond the standard model.

Unravelling the existence and the properties of such new physics requires experimental information complementary to the LHC. The muon $(g-2)$, together with searches for charged lepton flavor violation, electric dipole moments, and rare decays, belongs to a class of complementary low-energy experiments.

In fact, the muon magnetic moment has a special role because it is sensitive to a large class of models related and unrelated to EWSB and because it combines several properties in a unique way: it is a flavour- and CP-conserving, chirality-flipping and loop-induced quantity. In contrast, many high-energy collider observables at the LHC and a future linear collider are chirality-conserving, and many other low-energy precision observables are CP- or flavour-violating. These unique properties might be the reason why the muon $(g-2)$

is the only among the mentioned observables which shows a significant deviation between the experimental value and the SM prediction, see Eq. (2.27). Furthermore, while $g-2$ is sensitive to leptonic couplings, b- or K-physics more naturally probe the hadronic couplings of new physics. If charged lepton-flavor violation exists, observables such as $\mu \to e$ conversion can only determine a combination of the strength of lepton-flavor violation and the mass scale of new physics. In that case, $g-2$ can help to disentangle the nature of the new physics.

The role of $g-2$ as a discriminator between very different standard model extensions is well illustrated by a relation stressed by Czarnecki and Marciano [48]. It holds in a wide range of models as a result of the chirality-flipping nature of both $g-2$ and the muon mass: If a new physics model with a mass scale Λ contributes to the muon mass $\delta m_\mu(\text{N.P.})$, it also contributes to a_μ, and the two contributions are related as

$$a_\mu(\text{N.P.}) = \mathcal{O}(1) \times \left(\frac{m_\mu}{\Lambda}\right)^2 \times \left(\frac{\delta m_\mu(\text{N.P.})}{m_\mu}\right). \tag{2.28}$$

The ratio $C(\text{N.P.}) \equiv \delta m_\mu(\text{N.P.})/m_\mu$ cannot be larger than unity unless there is fine-tuning in the muon mass. Hence a first consequence of this relation is that new physics can explain the currently observed deviation (2.27) only if Λ is at the few-TeV scale or smaller.

In many models, the ratio C arises from one- or even two-loop diagrams, and is then suppressed by factors like $\alpha/4\pi$ or $(\alpha/4\pi)^2$. Hence, even for a given Λ, the contributions to a_μ are highly model dependent.

It is instructive to classify new physics models as follows:

- Models with $C(\text{N.P.}) \simeq 1$: Such models are of interest since the muon mass is essentially generated by radiative effects at some scale Λ. A variety of such models have been discussed in [48], including extended technicolor or generic models with naturally vanishing bare muon mass. For examples of radiative muon mass generation within supersymmetry, see e.g. [117, 118]. In these models the new physics contribution to a_μ can be very large,
$$a_\mu(\Lambda) \simeq \frac{m_\mu^2}{\Lambda^2} \simeq 1100 \times 10^{-11} \left(\frac{1\ \text{TeV}}{\Lambda}\right)^2. \tag{2.29}$$
and the difference Eq. (2.27) can be used to place a lower limit on the new physics mass scale, which is in the few TeV range [119, 118].

- Models with $C(\text{N.P.}) = \mathcal{O}(\alpha/4\pi)$: Such a loop suppression happens in many models with new weakly interacting particles like Z' or W', little Higgs or certain extra dimension models. As examples, the contributions to a_μ in a model with $\delta = 1$ (or 2) universal extra dimensions (UED) [120] and the Littlest Higgs model with T-parity (LHT) [121] are given by
$$a_\mu(\text{UED}) \simeq -5.8 \times 10^{-11}(1 + 1.2\delta) S_{\text{KK}}, \tag{2.30}$$
$$a_\mu(\text{LHT}) < 12 \times 10^{-11} \tag{2.31}$$
with $|S_{\text{KK}}| \lesssim 1$ [120]. A difference as large as Eq. (2.27) is very hard to accommodate unless the mass scale is very small, of the order of M_Z, which however is often excluded e.g. by LEP measurements. So typically these models predict very small contributions

to a_μ and will be disfavored if the current deviation will be confirmed by the new a_μ measurement.

Exceptions are provided by models where new particles interact with muons but are otherwise hidden from searches. An example is the model with a new gauge boson associated to a gauged lepton number $L_\mu - L_\tau$ [122], where a gauge boson mass of $\mathcal{O}(100\ \text{GeV})$ and large a_μ are viable; see however [123], which discusses a novel constraint that disfavors large contributions to a_μ in this model.

- Models with intermediate values for $C(\text{N.P.})$ and mass scales around the weak scale: In such models, contributions to a_μ could be as large as Eq. (2.27) or even larger, or smaller, depending on the details of the model. This implies that a more precise a_μ-measurement will have significant impact on such models and can even be used to measure model parameters. Supersymmetric (SUSY) models are the best known examples, so muon $g-2$ would have substantial sensitivity to SUSY particles. Compared to generic perturbative models, supersymmetry provides an enhancement to $C(\text{SUSY}) = \mathcal{O}(\tan\beta \times \alpha/4\pi)$ and to $a_\mu(\text{SUSY})$ by a factor $\tan\beta$ (the ratio of the vacuum expectation values of the two Higgs fields). Typical SUSY diagrams for the magnetic dipole moment, the electric dipole moment, and the lepton-number violating conversion process $\mu \to e$ in the field of a nucleus are shown pictorially in Fig. 2.10. The shown diagrams contain the SUSY partners of the muon, electron and the SM $\text{U}(1)_Y$ gauge boson, $\tilde{\mu}$, $\tilde{e}$, $\tilde{B}$. The full SUSY contributions involve also the SUSY partners to the neutrinos and all SM gauge and Higgs bosons. In a model with SUSY masses equal to Λ the SUSY contribution to a_μ is given by [124, 48, 125]

$$a_\mu(\text{SUSY}) \simeq \text{sgn}(\mu)\ 130 \times 10^{-11}\ \tan\beta\ \left(\frac{100\ \text{GeV}}{\Lambda}\right)^2 \tag{2.32}$$

which indicates the dependence on $\tan\beta$, and the SUSY mass scale, as well as the sign of the SUSY μ-parameter. The formula still approximately applies even if only the smuon and chargino masses are of the order Λ but e.g. squarks and gluinos are much heavier. However the SUSY contributions to a_μ depend strongly on the details of mass splittings between the weakly interacting SUSY particles (for details and the current status of the SUSY prediction for a_μ see e.g. [124, 125, 126, 127]). Thus muon $g-2$ is sensitive to SUSY models with SUSY masses in the few hundred GeV range, and it will help to measure SUSY parameters.

There are also non-supersymmetric models with similar enhancements. For instance, lepton flavor mixing can help. An example is provided in Ref. [129] by a model with two Higgs doublets and four generations, which can accommodate large Δa_μ without violating constraints on lepton flavor violation. In variants of Randall-Sundrum models [130, 131, 132] and large extra dimension models [133], large contributions to a_μ might be possible from exchange of Kaluza-Klein gravitons, but the theoretical evaluation is difficult because of cutoff dependences. A recent evaluation of the non-graviton contributions in Randall-Sundrum models, however, obtained a very small result [134].

Further examples include scenarios of unparticle physics [135, 136] (here a more precise a_μ-measurement would constrain the unparticle scale dimension and effective couplings), generic models with a hidden sector at the weak scale [137] or a model with

the discrete flavor symmetry group T' and Higgs triplets [138] (here a more precise a_μ-measurement would constrain hidden sector/Higgs triplet masses and couplings), or the model proposed in Ref. [139], which implements the idea that neutrino masses, leptogenesis and the deviation in a_μ all originate from dark matter particles. In the latter model, new leptons and scalar particles are predicted, and a_μ provides significant constraints on the masses and Yukawa couplings of the new particles.

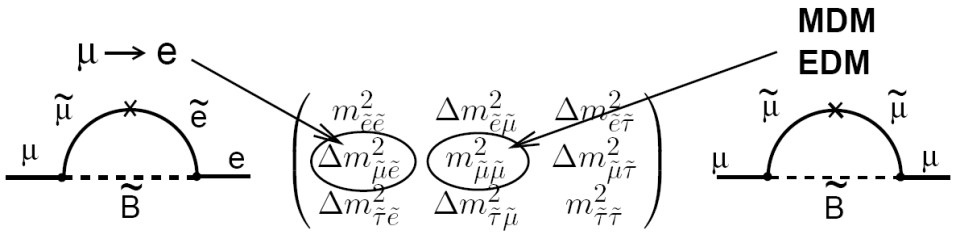

Figure 2.10: The SUSY contributions to the anomaly, and to $\mu \to e$ conversion, showing the relevant slepton mixing matrix elements. The MDM and EDM give the real and imaginary parts of the matrix element, respectively. The $\times$ indicates a chirality flip.

The following types of new physics scenarios are quite different from the ones above:

- Models with extended Higgs sector but without the $\tan\beta$-enhancement of SUSY models. Among these models are the usual two-Higgs-doublet models. The one-loop contribution of the extra Higgs states to a_μ is suppressed by two additional powers of the muon Yukawa coupling, corresponding to $a_\mu(\text{N.P.}) \propto m_\mu^4/\Lambda^4$ at the one-loop level. Two-loop effects from Barr-Zee diagrams can be larger [140], but typically the contributions to a_μ are negligible in these models.

- Models with additional light particles with masses below the GeV-scale, generically called dark sector models: Examples are provided by the models of Refs. [141, 142], where additional light neutral gauge bosons can affect electromagnetic interactions. Such models are intriguing since they completely decouple $g-2$ from the physics of EWSB, and since they are hidden from collider searches at LEP or LHC (see however Refs. [143, 144] for studies of possible effects at dedicated low-energy colliders and in Higgs decays at the LHC). They can lead to contributions to a_μ which are of the same order as the deviation in Eq. (2.27). Hence the new $g-2$ measurement will provide an important test of such models.

To summarize: many well-motivated models can accommodate larger contributions to a_μ — if any of these are realized $g-2$ can be used to constrain model parameters; many well-motivated new physics models give tiny contributions to a_μ and would be disfavored if the more precise $g-2$ measurement confirms the deviation in Eq. (2.27). There are also examples of models which lead to similar LHC signatures but which can be distinguished using $g-2$.

Models with large contributions to a_μ versus LHC data

We first focus on two particularly promising candidate models which could naturally explain a deviation as large as Eq. (2.27): dark sector models and SUSY models.

Dark sector models involve very light new particles with very weak interactions. They are constrained by other low-energy observables, such as $(g-2)$ of the electron, but there is a natural window in parameter space, where they can accommodate large contributions to a_μ. These models are hardly constrained by LHC data.

The situation is very different for SUSY models. SUSY searches are a central part of the LHC experiments and have not revealed any evidence for SUSY particles, so SUSY models are already strongly constrained by current LHC data. In the following we discuss why and how SUSY models are still compatible with large contributions to a_μ.

At the one-loop level, the diagrams of the minimal supersymmetric standard model (MSSM) involve the SUSY partners the gauge and Higgs bosons and the muon-neutrino and the muon, the so-called charginos, neutralinos and sneutrinos and smuons. The relevant parameters are the SUSY breaking mass parameters for the 2nd generation sleptons, the bino and wino masses M_2, M_1, and the Higgsino mass parameter μ. Strongly interacting particles, squarks and gluinos, and their masses are irrelevant on this level.

If all the relevant mass parameters are equal, the approximation (2.32) is valid, and the dominant contribution is from the chargino–sneutrino diagrams. If there are large mass splittings, the formula becomes inappropriate. For example, if μ is very large, the bino-like neutralino contribution of Fig. 2.10 is approximately linear in μ and can dominate. If there is a large mass splitting between the left- and right-handed smuon, even the sign can be opposite to Eq. (2.32), see the discussions in [124, 125, 126, 127].

On the two-loop level, further contributions exist which are typically subleading but can become important in regions of parameter space. For instance, there are diagrams without smuons or sneutrinos but with e.g. a pure chargino or stop loop [145, 146]. Such diagrams can even be dominant if first and second generation sfermions are very heavy, a scenario called effective SUSY.

Constraints from a_μ and LHC experiments and theoretical bias lead to the following conclusions:

- If supersymmetry is the origin of the deviation in a_μ, at least some SUSY particles cannot be much heavier than around 700 GeV (for $\tan\beta = 50$ or less), most favorably the smuons and charginos/neutralinos.

- The negative results of the LHC searches for SUSY particles imply lower limits of around 1 TeV on squark and gluino masses. However, the bounds are not model-independent but valid in scenarios with particular squark and gluino decay patterns.

- The constraint that a SM-like Higgs boson mass is around 125 GeV requires either very large loop corrections from large logarithms or non-minimal tree-level contributions from additional non-minimal particle content.

- The requirement of small fine-tuning between supersymmetry-breaking parameters and the Z-boson mass prefers certain particles, in particular stops, gluinos and Higgsinos to be rather light.

A tension between these constraints seems to be building up, but the constraints act on different aspects of SUSY models. Hence it is in principle no problem to accommodate all the experimental data in the general minimal supersymmetric standard model, for recent analyses see Refs. [147, 148]; for benchmark points representing different possible parameter regions see [127].

The situation is different in many specific scenarios, based e.g. on particular high-scale assumptions or constructed to solve a subset of the issues mentioned above. The Constrained MSSM (CMSSM) is one of the best known scenarios. Here, GUT-scale universality relates SUSY particle masses, in particular the masses of colored and uncolored sfermions of all generations. For a long time, many analyses have used a_μ as a central observable to constrain the CMSSM parameters, see e.g. [149]. The most recent analyses show that the LHC determination of the Higgs boson mass turns out to be incompatible with an explanation of the current Δa_μ within the CMSSM [150, 151, 152]. Hence, the CMSSM is already disfavored now, and it will be excluded if the future a_μ measurement confirms the current Δa_μ.

Likewise, in the so-called natural SUSY scenarios (see e.g. [156, 157]) the spectrum is such that fine-tuning is minimized while squarks and gluinos evade LHC bounds. These scenarios can explain the Higgs boson mass but fail to explain $g-2$ because of the heavy smuons.

On the other hand, the model of Ref. [153] is an example of a model with the aim to reconcile LHC-data, naturalness, and $g-2$. It is based on gauge-mediated SUSY breaking and extra vector-like matter, and it is naturally in agreement with FCNC constraints and the Higgs boson mass value. In this model the SUSY particles can be light enough to explain $g-2$, but in that case it is on the verge of being excluded by LHC data.

The rising tension between the constraints mentioned above, and further recent model-building efforts to solve it, are also reviewed in Refs. [154, 155]. In these references, more pragmatic approaches are pursued, and parameter regions within the general MSSM are suggested which are in agreement with all experimental constraints. All suggested regions have in common that they are split, i.e. some sparticles are much heavier than others. Ref. [154] suggests to focus on scenarios with light non-colored and heavy colored sparticles; Ref. [155] proposes split-family supersymmetry, where only the third family sfermions are very heavy. In both scenarios, $g-2$ can be explained, and the parameter space of interest can be probed by the next LHC run.

In the general model classification of the previous subsection the possibility of radiative muon mass generation was mentioned. This idea can be realized within supersymmetry, and it leads to SUSY scenarios quite different from the ones discussed so far. Since the muon mass at tree level is given by the product of a Yukawa coupling and the vacuum expectation value of the Higgs doublet H_d, there are two kinds of such scenarios. First, one can postulate that the muon Yukawa coupling is zero but chiral invariance is broken by soft supersymmetry-breaking A-terms. Then, the muon mass, and $a_\mu^{\rm SUSY}$, arise at the one-loop level and there is no relative loop suppression of $a_\mu^{\rm SUSY}$ [117, 118]. Second, one can postulate that the vacuum expectation value $\langle H_d \rangle$ is very small or zero [158, 159]. Then, the muon mass and $a_\mu^{\rm SUSY}$ arise at the one-loop level from loop-induced couplings to the other Higgs doublet. Both scenarios could accommodate large $a_\mu^{\rm SUSY}$ and TeV-scale SUSY particle masses.

Hence, in spite of the current absence of signals for new physics at the LHC, dark sector and SUSY models provide two distinct classes of models which are viable and can accom-

modate large contributions to a_μ. These examples of the CMSSM, natural SUSY, extended SUSY models, split MSSM scenarios, and radiative muon mass generation illustrate the model-dependence of $g-2$ within SUSY and its correlation to the other constraints. Clearly, a definitive knowledge of $a_\mu^{\rm SUSY}$ will be very beneficial for the interpretation of LHC data in terms of SUSY or any alternative new physics model.

a_μ and model selection and parameter measurement

The LHC is sensitive to virtually all proposed weak-scale extensions of the standard model, ranging from supersymmetry, extra dimensions and technicolor to little Higgs models, unparticle physics, hidden sector models and others. However, even if the existence of physics beyond the standard model is established, it will be far from easy for the LHC alone to identify which of these — or not yet thought of — alternatives is realized. Typically LHC data will be consistent with several alternative models.

The previous subsection has given examples of qualitatively different SUSY models which are in agreement with current LHC data. Even worse, even if in the future the LHC finds many new heavy particles which are compatible with SUSY, these new states might allow alternative interpretations in terms of non-SUSY models. In particular universal-extra-dimension models (UED) [160], or the Littlest Higgs model with T-parity (LHT) [161, 162] have been called "bosonic SUSY" since they can mimick SUSY but the partner particles have the opposite spin as the SUSY particles, see e.g. [163]. The muon $g-2$ would especially aid in the selection since UED or Littlest Higgs models predict a tiny effect to a_μ [120, 121], while SUSY effects are often much larger.

On the other hand, a situation where the LHC finds no physics beyond the standard model but the a_μ measurement establishes a deviation, might be a signal for dark sector models such as the secluded U(1) model [141], with new very weakly interacting light particles which are hard to identify at the LHC [143, 142, 144].

Next, if new physics is realized in the form of a non-renormalizable theory, a_μ might not be fully computable but depend on the ultraviolet cutoff. Randall-Sundrum or universal extra dimension models are examples of this situation. In such a case, the a_μ measurement will not only help to constrain model parameters but it will also help to get information on the ultraviolet completion of the theory.

The complementarity between a_μ and LHC can be exemplified quantitatively within general SUSY, because this is a well-defined and calculable framework. Fig. 2.11 illustrates the complementarity in selecting between different models.

The red points in the left plot in Fig. 2.11 show the values for the so-called SPS benchmark points [167] and new benchmark points E1, E4, NS1. The points E1, E4 are the split scenarios defined in Endo et al, Ref. [154] (cases (a) and (d) with $M_2 = 300$ GeV and $m_L = 500$ GeV), the point NS1 is the natural SUSY scenario defined in Ref. [156]. These points span a wide range and can be positive or negative, due to the factor sign(μ) in Eq. (2.32). The discriminating power of the current (yellow band) and an improved (blue band) measurement is evident from Fig. 2.11(a).

Even though several SPS points are actually experimentally excluded, their spread in Fig. 2.11(a) is still a good illustration of possible SUSY contributions to a_μ. E.g. the split scenarios of Refs. [154, 155] are comparable to SPS1b, both in their $g-2$ contribution and

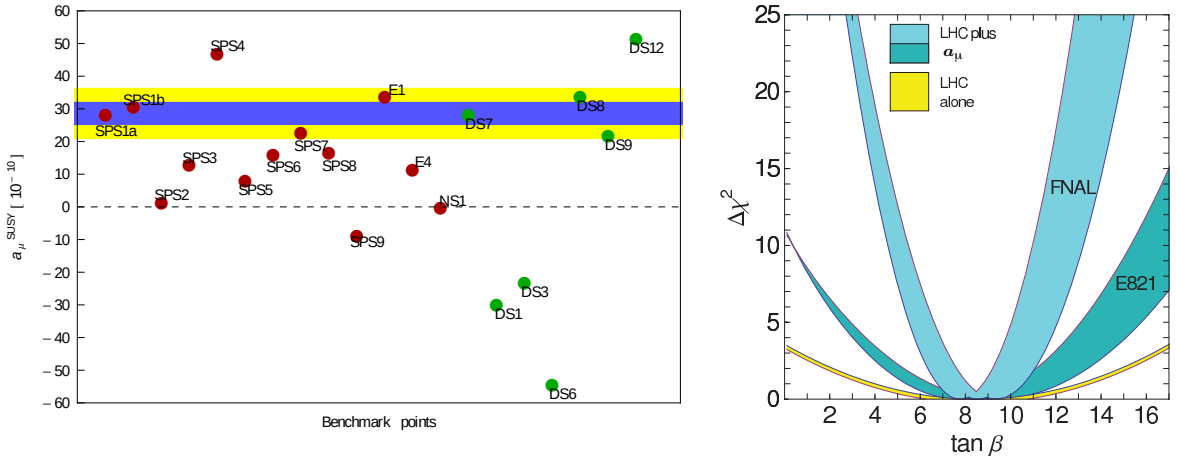

(a) (b)

Figure 2.11: (a) SUSY contributions to a_μ for the SPS and other benchmark points (red), and for the "degenerate solutions" from Ref. [164]. The yellow band is the $\pm 1\ \sigma$ error from E821, the blue is the projected sensitivity of E989. (b) Possible future $\tan\beta$ determination assuming that a slightly modified MSSM point SPS1a (see text) is realized. The bands show the $\Delta\chi^2$ parabolas from LHC-data alone (yellow) [166], including the a_μ with current precision (dark blue) and with prospective precision (light blue). The width of the blue curves results from the expected LHC-uncertainty of the parameters (mainly smuon and chargino masses) [166].

in the relevant mass spectrum. Natural SUSY is similar to SPS2, which corresponds to a heavy sfermion scenario. Similarly, the "supersymmetry without prejudice" study of Ref. [168] confirmed that the entire range $a_\mu^{\rm SUSY} \sim (-100 \ldots + 300) \times 10^{-11}$ was populated by a reasonable number of "models" which are in agreement with other experimental constraints. Therefore, a precise measurement of $g-2$ to $\pm 16 \times 10^{-11}$ will be a crucial way to rule out a large fraction of models and thus determine SUSY parameters.

One might think that if SUSY exists, the LHC-experiments will find it and measure its parameters. Above it has been mentioned that SUSY can be mimicked by "bosonic SUSY" models. The green points in Fig. 2.11(a) illustrate that even within SUSY, certain SUSY parameter points can be mimicked by others. The green points correspond to "degenerate solutions" of Ref. [164] — different SUSY parameter points which cannot be distinguished at the LHC alone (see also Ref. [165] for the LHC inverse problem). Essentially the points differ by swapping the values and signs of the SUSY parameters μ, M_1, M_2. They have very different a_μ predictions, and hence a_μ can resolve such LHC degeneracies.

The right plot of Fig. 2.11 illustrates that the SUSY parameter $\tan\beta$ can be measured more precisely by combining LHC-data with a_μ. It is based on the assumption that SUSY is realized, found at the LHC and the origin of the observed a_μ deviation (2.27). To fix an example, we use a slightly modified SPS1a benchmark point with $\tan\beta$ scaled down to $\tan\beta = 8.5$ such that $a_\mu^{\rm SUSY}$ is equal to an assumed deviation $\Delta a_\mu = 255 \times 10^{-11}$.[7] Ref.

[7]The actual SPS1a point is ruled out by LHC; however for our purposes only the weakly interacting

[166] has shown that then mass measurements at the LHC alone are sufficient to determine $\tan\beta$ to a precision of ± 4.5 only. The corresponding $\Delta\chi^2$ parabola is shown in yellow in the plot. In such a situation one can study the SUSY prediction for a_μ as a function of $\tan\beta$ (all other parameters are known from the global fit to LHC data) and compare it to the measured value, in particular after an improved measurement. The plot compares the LHC $\Delta\chi^2$ parabola with the ones obtained from including a_μ, $\Delta\chi^2 = [(a_\mu^{\rm SUSY}(\tan\beta) - \Delta a_\mu)/\delta a_\mu]^2$ with the errors $\delta a_\mu = 80 \times 10^{-11}$ (dark blue) and 34×10^{-11} (light blue). As can be seen from the Figure, using today's precision for a_μ would already improve the determination of $\tan\beta$, but the improvement will be even more impressive after the future a_μ measurement.

One should note that even if better ways to determine $\tan\beta$ at the LHC alone might be found, an independent determination using a_μ will still be highly valuable, as $\tan\beta$ is one of the central MSSM parameters; it appears in all sectors and in almost all observables. In non-minimal SUSY models the relation between $\tan\beta$ and different observables can be modified. Therefore, measuring $\tan\beta$ in different ways, e.g. using certain Higgs- or b-decays at the LHC or at b-factories and using a_μ, would constitute a non-trivial and indispensable test of the universality of $\tan\beta$ and thus of the structure of the MSSM.

In summary, the anomalous magnetic moment of the muon is sensitive to contributions from a wide range of physics beyond the standard model. It will continue to place stringent restrictions on all of the models, both present and yet to be written down. If physics beyond the standard model is discovered at the LHC or other experiments, a_μ will constitute an indispensable tool to discriminate between very different types of new physics, especially since it is highly sensitive to parameters which are difficult to measure at the LHC. If no new phenomena are found elsewhere, then it represents one of the few ways to probe physics beyond the standard model. In either case, it will play an essential and complementary role in the quest to understand physics beyond the standard model at the TeV scale.

---

particles are relevant, and these are not excluded. The following conclusions are neither very sensitive to the actual $\tan\beta$ value nor to the actual value of the deviation Δa_μ.

References

[1] O. Stern, Z. Phys. **7**, 249 (1921);

[2] W. Gerlach and O. Stern, , Z. Phys. **8**, 110 (1922); Z. Phys. **9** and 349(1922), Z. Phys. **9**, 353 (1924); W. Gerlach and O. Stern, Ann. Phys. **74**, 673 (1924).

[3] G.E. Uhlenbeck and S. Goudsmit, Naturwissenschaften **47**, 953 (1925); G.E. Uhlenbeck and S. Goudsmit, Nature **117** (1926) 264.

[4] E. Schrödinger, Ann. Phys. **79** (1926) 361.

[5] L.H. Thomas, Nature **117**, (1926) 514 and Phil. Mag. **3** (1927) 1.

[6] T.E. Phipps and J.B. Taylor, Phys. Rev. **29**, 309 (1927).

[7] P.A.M. Dirac, Proc. R. Soc. (London) **A117**, 610 (1928), and **A118**, 351 (1928). See also, P.A.M. Dirac, *The Principles of Quantum Mechanics*, 4th edition, Oxford University Press, London, 1958.

[8] Sin-itiro Tomonaga, *The Story of Spin*, translated by Takeshi Oka, U. Chicago Press, 1997.

[9] R. Frisch and O. Stern, Z. Phys. **85**, 4 (1933), and I. Estermann and O. Stern, Z. Phys. **85**, 17 (1933).

[10] Luis W. Alvarez and F. Bloch, Phys. Rev. **57**, 111 (1940).

[11] J.E. Nafe, E.B. Nelson and I.I. Rabi Phys. Rev. **71**, 914(1947).

[12] D.E. Nagel, R.S. Julian and J.R. Zacharias, Phys. Rev. **72**, 971 (1947).

[13] P. Kusch and H.M Foley, Phys. Rev **72**, 1256 (1947).

[14] Hans A. Bethe and Edwin E. Salpeter, *Quantum Mechanics of One- and Two-Electron Atoms*, Springer-Verlag, (1957), p. 51.

[15] See Figure 5 in Paul Kunze, Z. Phys. **83**, 1 (1933).

[16] Carl D. Anderson and Seth H. Neddermeyer, Phys. Rev. **50** (1936) 263, and Seth H. Neddermeyer and Carl D. Anderson, Phys. Rev. **51** (1937) 844.

[17] J.C. Street, E.C. Stevenson, Phys. Rev. **52** (1937) 1003.

[18] Y. Nishina, M. Tekeuchi and T. Ichimiya, Phys. Rev. **52** (1937) 1198.

[19] M.M. Jean Crussard and L. Leprince-Ringuet, Compt. Rend. **204** (1937) 240.

[20] Garwin RL, Lederman LM, Weinrich M, Phys. Rev. 105:1415 (1957)

[21] J.I. Friedman and V.L. Telegdi, Phys. Rev. **105**, 1681 (1957).

[22] Garwin RL, Hutchinson DP, Penman S, Shapiro G, Phys. Rev. 118:271 (1960)

[23] Charpak G, et al. Phys. Rev. Lett. 6:28 (1961), Nuovo Cimento. 22:1043 (1961), Phys. Lett. 1:16 (1962), Nuovo Cimento. 37:1241 (1965) and Charpak G. et al. Phys. Lett. 1:16 (1962)

[24] Bailey J, et al. Phys. Lett. 28B:287 (1968). Additional details can be found in Bailey J, et al. Nuovo Cimento. A9:369 (1972) and references therein.

[25] Bailey J, et al. Nucl. Phys. B150:1 (1979)

[26] E.M. Purcell and N.F. Ramsey, Phys. Rev. **78**, 807 (1950).

[27] T.D. Lee and C.N. Yang, Phys. Rev. **104** (1956) 254.

[28] J.H. Smith, E.M. Purcell and N.F. Ramsey, Phys. Rev. **108**, 120 (1957).

[29] L. Landau, Nucl. Phys. **3**, 127 (1957).

[30] N.F. Ramsey Phys. Rev. **109**, 225 (1958).

[31] W.C. Griffith, et al., Phys. Rev. Lett. **102**, 101601 (2009).

[32] C.A. Baker, et al., Phys. Rev. Lett. **97**, 131801 (2006).

[33] J.J. Hudson, et al., Nature **473**, 493 (2011).

[34] G.W. Bennett, et al., Phys. Rev. **D 80**, 052008 (2009).

[35] Bargmann V, Michel L, Telegdi VL, Phys. Rev. Lett. 2:435 (1959)

[36] Bennett GW, et al. (The $g-2$ Collab.) Phys. Rev. Lett. 92:161802 (2004)

[37] Bennett GW, et al.(The $g-2$ Collab.) Phys. Rev. D, 73:072003 (2006)

[38] The $g-2$ Collaboration: R.M. Carey et al., Phys. Rev. Lett. **82**, 1632 (1999).

[39] The $g-2$ Collaboration: H.N. Brown et al., Phys. Rev. D **62**, 091101 (2000).

[40] The $g-2$ Collaboration: H.N. Brown et al., Phys. Rev. Lett. **86**, 2227 (2001).

[41] The $g-2$ Collaboration: G.W. Bennett et al., Phys. Rev. Lett. **89**, 101804 (2002); Erratum-ibid. **89**, 129903 (2002).

[42] C.S. Wu, E. Ambler, R.W. Hayward, D.D. Hoppes, R.P. Hudson, Phys. Rev. **105**, 1413 (1957).

[43] Mohr PJ, Taylor BN, Newell DB, (CODATA recommended values). *Rev. Mod. Phys.* 80:633 (2008)

[44] R. Prigl, *et al.*, Nucl. Inst. Methods Phys. Res. **A374** 118 (1996).

[45] W. Liu et al., Phys. Rev. Lett. **82**, 711 (1999).

[46] Topical Workshop on The Muon Magnetic Dipole Moment; Oct. 2007 School of Physics and Astronomy, The University of Glasgow. See: www.ippp.dur.ac.uk/old/MuonMDM/.

[47] T. Kinoshita and W.J. Marciano in *Quantum Electrodynamics* (Directions in High Energy Physics, Vol. 7), ed. T. Kinoshita, (World Scientific, Singapore, 1990), p. 419.

[48] Andrzej Czarnecki and William J. Marciano, Phys. Rev. **D64** 013014 (2001).

[49] Xu Feng, Karl Jansen, Marcus Perschlies and Dru B. Renner, Phys. Rev. Lett. 107 081802 (2011).

J. Phys.G G 34:R45 (2007)

[50] Thomas Blum, Achim Denig, Ivan Logashenko, Eduardo de Rafael, B. Lee Roberts, Thomas Teubner and Graziano Venanzoni, arXiv:1311.2198v1 [hep-ph] 9 Nov 2013.

[51] J. Schwinger, Phys. Rev. **73** (1948) 416, and Phys. Rev. **76** (1949) 790. The former paper contains a misprint in the expression for a_e that is corrected in the longer paper.

[52] T. Aoyama, M. Hayakawa, T. Kinoshita and M. Nio, Phys. Rev. Lett. **109** (2012) 111808.

[53] J. P. Miller, E. de Rafael, B. L. Roberts and D. Stöckinger, Ann. Rev. Nucl. Part. Sci. **62** (2012) 237.

[54] D. Stöckinger, in Advanced Series on Directions in High Energy Physics - Vol. 20 *Lepton Dipole Moments*, eds. B. L. Roberts and W. J. Marciano, World Scientific (2010), p.393.

[55] D. Hanneke, S. Fogwell and G. Gabrielse, Phys. Rev. Lett. **100** (2008) 120801.

[56] M. Davier, in Advanced Series on Directions in High Energy Physics - Vol. 20 *Lepton Dipole Moments*, eds. B. L. Roberts and W. J. Marciano, World Scientific (2010), chapter 8.

[57] R. Bouchendira, P. Clade, S. Guellati-Khelifa, F. Nez and F. Biraben, Phys. Rev. Lett. **106** (2011) 080801.

[58] A. Czarnecki, B. Krause and W. J. Marciano, Phys. Rev. Lett. **76** (1996) 3267.

[59] S. Peris, M. Perrottet and E. de Rafael, Phys. Lett. **B355** (1995) 523.

[60] A. Czarnecki, B. Krause and W. Marciano, Phys. Rev. **D52** (1995) 2619.

[61] A. Czarnecki, W. J. Marciano and A. Vainshtein, Phys. Rev. **D67** (2003) 073006, Erratum-ibid. **D73** (2006) 119901.

[62] S. Heinemeyer, D. Stöckinger and G. Weiglein, Nucl. Phys. B **699**, 103 (2004) [hep-ph/0405255].

[63] T. Gribouk and A. Czarnecki, Phys. Rev. D **72**, 053016 (2005) [hep-ph/0509205].

[64] A. Czarnecki and W. J. Marciano, in Advanced Series on Directions in High Energy Physics - Vol. 20 *Lepton Dipole Moments*, eds. B. L. Roberts and W. J. Marciano, World Scientific (2010), p. 11, and references therein.

[65] C. Gnendiger, D. Stöckinger and H. Stöckinger-Kim, Phys. Rev. **D88** (2013) 053005.

[66] W. A. Bardeen, R. Gastmans and B. Lautrup, Nucl. Phys. **B46** (1972) 319; R. Jackiw and S. Weinberg, Phys. Rev. **D5** (1972) 157; I. Bars and M. Yoshimura, Phys. Rev. **D6** (1972) 374; K. Fujikawa, B. W. Lee and A. I. Sanda, Phys. Rev. **D6** (1972) 2923.

[67] J. P. Miller, E. de Rafael and B. L. Roberts, Rept. Prog. Phys. **70** (2007) 795.

[68] M. Knecht, S. Peris, M. Perrottet and E. de Rafael, JHEP **0211** (2002) 003.

[69] A. Vainshtein, Phys. Lett. **B569** (2003) 187.

[70] M. Knecht, S. Peris, M. Perrottet and E. de Rafael, JHEP **0403** (2004) 035.

[71] M. Davier, A. Hoecker, B. Malaescu and Z. Zhang, Eur. Phys. J. **C71** (2011) 1515, Erratum-ibid. **C72** (2012) 1874.

[72] K. Hagiwara, R. Liao, A. D. Martin, D. Nomura and T. Teubner, J. Phys. **G38** (2011) 085003.

[73] K. Hagiwara, A. D. Martin, D. Nomura and T. Teubner, Phys. Lett. **B649** (2007) 173.

[74] M. Davier,Nucl. Phys. Proc. Suppl. **169** (2007) 288.

[75] F. Jegerlehner and A. Nyffeler, Phys.Rept. **477** (2009) 1.

[76] R. Alemany, M. Davier and A. Höcker, Eur. Phys. J. **C2** (1998) 123.

[77] F. Jegerlehner and R. Szafron, Eur. Phys. J. **C71** (2011) 1632.

[78] M. Benayoun, P. David, L. DelBuono and F. Jegerlehner, Eur. Phys. J. **C72** (2012) 1848.

[79] M. Benayoun, P. David, L. DelBuono and F. Jegerlehner, Eur. Phys. J. **C73** (2013) 2453.

[80] A. Kurz, T. Liu, P. Marquard and M. Steinhauser, arXiv:1403.6400 [hep-ph].

[81] M. Knecht, A. Nyffeler, M. Perrottet and E. de Rafael, Phys. Rev. Lett. **88** (2002) 071802.

[82] K. Melnikov and A. Vainshtein, Phys. Rev. **D70** (2004) 113006.

[83] J. Prades, E. de Rafael and A. Vainshtein, in Advanced Series on Directions in High Energy Physics - Vol. 20 *Lepton Dipole Moments*, eds. B. L. Roberts and W. J. Marciano, World Scientific (2010), p. 303; and arXiv:0901.0306v1 [hep-ph].

[84] A. Nyffeler, Phys. Rev. **D79** (2009) 073012.

[85] http://www.int.washington.edu/PROGRAMS/11-47w/

[86] https://indico.mitp.uni-mainz.de/conferenceDisplay.py?confId=13

[87] T. Goecke, C. S. Fischer and R. Williams, Phys. Rev. **D83** (2011) 094006, Erratum-ibid. **D86** (2012) 099901; Phys. Rev. **D87** (2013) 034013.

[88] G. Colangelo, M. Hoferichter, M. Procura and P. Stoffer, arXiv:1402.7081 [hep-ph].

[89] S. Eidelman and F. Jegerlehner, Z. Phys. **C67** (1995) 585.

[90] R. R. Akhmetshin et al. (CMD2 Collaboration), Phys. Lett. **B527** (2002) 161.

[91] M. Davier, S. Eidelman, A. Höcker and Z. Zhang, Eur. Phys. J. **C27** (2003) 497.

[92] K. Hagiwara, A. D. Martin, D. Nomura and T. Teubner, Phys. Rev. **D69** (2004) 093003.

[93] F. Jegerlehner, Nucl. Phys. Proc. Suppl. **181-182** (2008) 26.

[94] F. Burger, X. Feng, G. Hotzel, K. Jansen, M. Petschlies and D. B. Renner, arXiv:1308.4327 [hep-lat].

[95] M. Della Morte, B. Jager, A. Juttner and H. Wittig, PoS LATTICE **2012** (2012) 175 [arXiv:1211.1159 [hep-lat]].

[96] T. Blum, M. Hayakawa and T. Izubuchi, PoS LATTICE **2012** (2012) 022 [arXiv:1301.2607 [hep-lat]].

[97] P. Boyle, L. Del Debbio, E. Kerrane and J. Zanotti, Phys. Rev. **D85** (2012) 074504.

[98] C. Aubin and T. Blum, Phys. Rev. **D75** (2007) 114502.

[99] G. M. de Divitiis, R. Petronzio and N. Tantalo, Phys. Lett. **B718** (2012) 589.

[100] T. Blum, T. Izubuchi and E. Shintani, arXiv:1208.4349 [hep-lat].

[101] C. Aubin, T. Blum, M. Golterman and S. Peris, Phys. Rev. **D86** (2012) 054509.

[102] X. Feng, S. Hashimoto, G. Hotzel, K. Jansen, M. Petschlies and D. B. Renner, Phys. Rev. **D88** (2013) 034505.

[103] C. Aubin, T. Blum, M. Golterman and S. Peris, arXiv:1307.4701 [hep-lat].

[104] G. Amelino-Camelia et al. (KLOE-2 Collaboration), Eur. Phys. J. **C68** (2010) 619.

[105] D. Babusci, H. Czyz, F. Gonnella, S. Ivashyn, M. Mascolo, R. Messi, D. Moricciani and A. Nyffeler et al., Eur. Phys. J. **C72** (2012) 1917.

[106] F. Jegerlehner, Acta Phys. Polon. **B38** (2007) 3021; *The anomalous magnetic moment of the muon*, Springer (2008).

[107] M. Knecht and A. Nyffeler, Eur. Phys. J. **C21** (2001) 659.

[108] K. Nakamura et al., J. Phys. **G37** (2010) 075021.

[109] A. Nyffeler, PoS **CD09** (2009) 080 [arXiv:0912.1441 [hep-ph]].

[110] I. Larin et al., Phys. Rev. Lett. **106** (2011) 162303.

[111] F. Archilli et al., Nucl. Instrum. Meth. **A617** (2010) 266.

[112] D. Babusci et al., Eur. Phys. J. **C72** (2012) 1917.

[113] H. Czyż and S. Ivashyn, Comput. Phys. Commun. **182** (2011) 1338.

[114] H. J. Behrend et al., Z. Phys. **C49** (1991) 401; J. Gronberg et al., Phys. Rev. **D57** (1998) 33.

[115] D. W. Hertzog, J. P. Miller, E. de Rafael, B. Lee Roberts and D. Stöckinger, arXiv:0705.4617 [hep-ph].

[116] The articles listed in the SPIRES citations to Ref. [40] contain many different models beyond the standard model.

[117] F. Borzumati, G. R. Farrar, N. Polonsky and S. D. Thomas, Nucl. Phys. B **555** (1999) 53 [hep-ph/9902443].

[118] A. Crivellin, J. Girrbach and U. Nierste, Phys. Rev. D **83** (2011) 055009 [arXiv:1010.4485 [hep-ph]].

[119] E. Eichten, et al., Phys. Rev. Lett. **45**, 225 (1980); K. Lane, arXiv [hep-ph/0102131].

[120] T. Appelquist and B. A. Dobrescu, Phys. Lett. B **516** (2001) 85 [arXiv:hep-ph/0106140].

[121] M. Blanke, A. J. Buras, B. Duling, A. Poschenrieder and C. Tarantino, JHEP **0705** (2007) 013 [arXiv:hep-ph/0702136].

[122] S. Baek, N. G. Deshpande, X. G. He and P. Ko, Phys. Rev. D **64**, 055006 (2001) [hep-ph/0104141]; E. Ma, D. P. Roy and S. Roy, Phys. Lett. B **525** (2002) 101 [hep-ph/0110146]; J. Heeck and W. Rodejohann, Phys. Rev. D **84** (2011) 075007 [arXiv:1107.5238 [hep-ph]].

[123] W. Altmannshofer, S. Gori, M. Pospelov and I. Yavin, arXiv:1403.1269 [hep-ph].

[124] T. Moroi, Phys. Rev. D **53** (1996) 6565 [Erratum-ibid. **56** (1997) 4424].

[125] D. Stöckinger, J. Phys. G **34** (2007) R45 [arXiv:hep-ph/0609168].

[126] G. -C. Cho, K. Hagiwara, Y. Matsumoto and D. Nomura, JHEP **1111**, 068 (2011) [arXiv:1104.1769 [hep-ph]].

[127]

[128] H. G. Fargnoli, C. Gnendiger, S. Paßehr, D. Stöckinger and H. Stöckinger-Kim, Phys. Lett. B **726**, 717 (2013) [arXiv:1309.0980 [hep-ph]]; JHEP **1402**, 070 (2014) [arXiv:1311.1775 [hep-ph]].

[129] S. Bar-Shalom, S. Nandi and A. Soni, Phys. Lett. B **709**, 207 (2012) [arXiv:1112.3661 [hep-ph]].

[130] H. Davoudiasl, J. L. Hewett and T. G. Rizzo, Phys. Lett. B **493** (2000) 135 [arXiv:hep-ph/0006097].

[131] S. C. Park and H. S. Song, Phys. Lett. B **506** (2001) 99 [arXiv:hep-ph/0103072].

[132] C. S. Kim, J. D. Kim and J. H. Song, Phys. Lett. B **511** (2001) 251 [arXiv:hep-ph/0103127].

[133] M. L. Graesser, Phys. Rev. D **61** (2000) 074019 [arXiv:hep-ph/9902310].

[134] M. Beneke, P. Dey and J. Rohrwild, JHEP **1308**, 010 (2013) [arXiv:1209.5897 [hep-ph]]. M. Beneke, P. Moch and J. Rohrwild, arXiv:1404.7157 [hep-ph].

[135] K. Cheung, W. Y. Keung and T. C. Yuan, Phys. Rev. Lett. **99** (2007) 051803 [arXiv:0704.2588 [hep-ph]].

[136] J. A. Conley and J. S. Gainer, arXiv:0811.4168 [hep-ph].

[137] D. McKeen, arXiv:0912.1076 [hep-ph].

[138] C. M. Ho and T. W. Kephart, Phys. Lett. B **687**, 201 (2010) [arXiv:1001.3696 [hep-ph]].

[139] T. Hambye, K. Kannike, E. Ma and M. Raidal, Phys. Rev. D **75** (2007) 095003 [arXiv:hep-ph/0609228].

[140] M. Krawczyk, Acta Phys. Polon. B **33**, 2621 (2002) [hep-ph/0208076].

[141] M. Pospelov, Phys. Rev. D **80** (2009) 095002 [arXiv:0811.1030 [hep-ph]].

[142] H. Davoudiasl, H. -S. Lee and W. J. Marciano, Phys. Rev. Lett. **109**, 031802 (2012) [arXiv:1205.2709 [hep-ph]].

[143] R. Essig, P. Schuster and N. Toro, Phys. Rev. D **80** (2009) 015003 [arXiv:0903.3941 [hep-ph]].

[144] H. Davoudiasl, H. -S. Lee and W. J. Marciano, Phys. Rev. D **86**, 095009 (2012) [arXiv:1208.2973 [hep-ph]].

[145] S. Heinemeyer, D. Stöckinger and G. Weiglein, Nucl. Phys. B **690** (2004) 62 [arXiv:hep-ph/0312264]; S. Heinemeyer, D. Stöckinger and G. Weiglein, Nucl. Phys. B **699** (2004) 103 [arXiv:hep-ph/0405255].

[146] A. Arhrib and S. Baek, Phys. Rev. D **65**, 075002 (2002) [hep-ph/0104225].

[147] R. Benbrik, M. Gomez Bock, S. Heinemeyer, O. Stal, G. Weiglein and L. Zeune, Eur. Phys. J. C **72**, 2171 (2012) [arXiv:1207.1096 [hep-ph]].

[148] A. Arbey, M. Battaglia, A. Djouadi and F. Mahmoudi, JHEP **1209**, 107 (2012) [arXiv:1207.1348 [hep-ph]].

[149] R. Ruiz de Austri, R. Trotta and L. Roszkowski, JHEP **0605** (2006) 002 [arXiv:hep-ph/0602028]; JHEP **0704** (2007) 084 [arXiv:hep-ph/0611173]; JHEP **0707** (2007) 075 [arXiv:0705.2012]; B. C. Allanach, C. G. Lester and A. M. Weber, JHEP **0612** (2006) 065; B. C. Allanach, K. Cranmer, C. G. Lester and A. M. Weber, JHEP **0708**, 023 (2007); J. R. Ellis, S. Heinemeyer, K. A. Olive, A. M. Weber and G. Weiglein, JHEP **0708** (2007) 083; S. Heinemeyer, X. Miao, S. Su and G. Weiglein, JHEP **0808**, 087 (2008).

[150] P. Bechtle, T. Bringmann, K. Desch, H. Dreiner, M. Hamer, C. Hensel, M. Kramer and N. Nguyen *et al.*, JHEP **1206**, 098 (2012) [arXiv:1204.4199 [hep-ph]].

[151] C. Balazs, A. Buckley, D. Carter, B. Farmer and M. White, arXiv:1205.1568 [hep-ph].

[152] O. Buchmueller, R. Cavanaugh, M. Citron, A. De Roeck, M. J. Dolan, J. R. Ellis, H. Flacher and S. Heinemeyer *et al.*, Eur. Phys. J. C **72**, 2243 (2012) [arXiv:1207.7315 [hep-ph]].

[153] M. Endo, K. Hamaguchi, S. Iwamoto, K. Nakayama and N. Yokozaki, Phys. Rev. D **85** (2012) 095006 [arXiv:1112.6412 [hep-ph]].

[154] M. Endo, K. Hamaguchi, S. Iwamoto and T. Yoshinaga, arXiv:1303.4256 [hep-ph].

[155] M. Ibe, T. T. Yanagida and N. Yokozaki, arXiv:1303.6995 [hep-ph].

[156] H. Baer, V. Barger, P. Huang and X. Tata, JHEP **1205** (2012) 109 [arXiv:1203.5539 [hep-ph]].

[157] M. Papucci, J. T. Ruderman and A. Weiler, JHEP **1209**, 035 (2012) [arXiv:1110.6926 [hep-ph]].

[158] B. A. Dobrescu and P. J. Fox, Eur. Phys. J. C **70** (2010) 263 [arXiv:1001.3147 [hep-ph]].

[159] W. Altmannshofer and D. M. Straub, JHEP **1009** (2010) 078 [arXiv:1004.1993 [hep-ph]].

[160] T. Appelquist, H. -C. Cheng and B. A. Dobrescu, Phys. Rev. D **64**, 035002 (2001) [hep-ph/0012100].

[161] I. Low, JHEP **0410**, 067 (2004) [hep-ph/0409025].

[162] J. Hubisz and P. Meade, Phys. Rev. D **71**, 035016 (2005) [hep-ph/0411264].

[163] J. M. Smillie and B. R. Webber, JHEP **0510** (2005) 069 [arXiv:hep-ph/0507170].

[164] Adam C, Kneur J -L, Lafaye R, Plehn T, Rauch M, Zerwas D. *Eur. Phys. J. C* 71:1520 (2011) [arXiv:1007.2190 [hep-ph]]

[165] N. Arkani-Hamed, G. L. Kane, J. Thaler and L. T. Wang, JHEP **0608**, 070 (2006) [arXiv:hep-ph/0512190].

[166] M. Alexander, S. Kreiss, R. Lafaye, T. Plehn, M. Rauch, and D. Zerwas, Chapter 9 in M. M. Nojiri *et al.*, *Physics Beyond the Standard Model: Supersymmetry,* arXiv:0802.3672 [hep-ph].

[167] B. C. Allanach *et al.*, *Proc. of the APS/DPF/DPB Summer Study on the Future of Particle Physics (Snowmass 2001)* ed. N. Graf, Eur. Phys. J. C **25** (2002) 113 [eConf **C010630** (2001) P125].

[168] C. F. Berger, J. S. Gainer, J. L. Hewett and T. G. Rizzo, JHEP **0902**, 023 (2009) [arXiv:0812.0980 [hep-ph]].